

G_3 - interacting scalar tensor dark energy

Masroor C. Pookkillath^{1,*} and Nandan Roy^{1,†}

¹*Centre for Theoretical Physics and Natural Philosophy, Mahidol University,
Nakhonsawan Campus, Phayuha Khiri, Nakhonsawan 60130, Thailand*

We study the effect of adding an interaction in the G_3 term of Horndeski theory, where the propagation of gravitational waves are not modified. We derive the background and perturbation equations of motion from the action. We also derive the no-ghost and Laplacian instability conditions for tensor modes and scalar mode propagation. Then we study the evolution of the matter perturbation in the quasi-static approximation. We find that the gravitational couplings to the baryonic and cold dark matter over density are modified in this theory. We introduce a concrete model of the free function in the theory and study the background and linear perturbation dynamics. We then use the genetic algorithm to test the model. We compare the $H(z)$ function of the model and the $H(z)$ curve predicted by the genetic algorithm, using the $H(z)$ data. For the perturbation sector we compute the $f\sigma_8$ observable for the model and compare it with the predicted function from the genetic algorithm from the $f\sigma_8$ data.

I. INTRODUCTION

In the Λ CDM description of the universe, the cosmological constant Λ is introduced to the Einstein-Hilbert action to explain the observed cosmic expansion today and it has a constant equation of state $w_\Lambda = -1$. In addition, a fluid component with zero pressure (zero temperature, hence cold) is considered to explain the cold dark matter component. Even though the Λ CDM model is favored by existing cosmological data [1–7], it fails to fully explain the cosmic expansion in late-time cosmology, the dark energy problem, and to provide an adequate description for cold dark matter. Additionally, the model struggles with several theoretical challenges, such as the cosmological constant problem, fine-tuning problem, and more. On top of the theoretical incompleteness of the Λ CDM model, there are growing tensions that began to appear after the 2013 release of data from the Planck mission [6].

The value of the Hubble expansion rate today, H_0 inferred from the Planck Cosmic Microwave Background 2013 data is reported to be significantly lower than the value measured from the Type Ia supernovae [8]. Over the years, this tension keeps increasing. Currently, the Planck–2018 result shows that the value of the current acceleration rate of the universe is $67.4 \pm 0.5 \text{ km s}^{-1} \text{ Mpc}^{-1}$ [7]. But from the local measurement from the SH0ES Collaboration, it is reported that the value of the present accelerated expansion is $74.1 \pm 1 \text{ km s}^{-1} \text{ Mpc}^{-1}$ [9]. This adds up to a tension of around 5σ and is called the Hubble tension.

Another noticeable tension or discrepancy is in the estimation of the parameter $\sigma_8(S_8)$, which measures the density of the fluctuation, that resulted in the formation of the structures that we see today. This parameter estimated from the cosmic microwave background radiation [7], is higher than that measured from the Large scale structure data [10], which results in a 3σ discrepancy. These tensions in the estimation of major cosmological parameters from different kinds of observations suggest that the physics of the dark sectors of the universe might be different from the Λ CDM model.

The dynamic nature of dark energy is one of the alternatives to the cosmological constant which can help us to alleviate the current tensions. Modified theories of gravity are successful in giving a dynamical nature to the dark energy and dark matter phenomenon. For example, the quintessence model is introduced to explain the late-time cosmic expansion with a scalar field, instead of trivial cosmological constant Λ [11]¹. Later this model was generalised to more general theories of scalar-tensor gravity, like k -essence [19], Horndeski gravity [20], beyond Horndeski [21] and DHOST theories [22]. Vector-tensor theory is also introduced to explain the dynamical dark energy, for example [23]. Vector-tensor dark energy was also generalised to a Generalised Proca theory [24], further extended to Proca-Nuevo [25]. The cosmology of vector-tensor theories are studied in [26–28]. The dark energy models with scalar field and the vector field were extended to interaction with cold dark matter. In the literature, the interaction is usually introduced with phenomenological approach. In [29] a general Lagrangian for the interacting scalar field dark energy and dark matter is introduced, in which an interaction term is $\partial_\mu \phi u^\mu$, where u^μ is the four

* masroor.cha@mahidol.ac.th

† nandan.roy@mahidol.ac.th

¹ There are also other models that can mimic the dark energy phenomenon, with out introducing any additional degrees of freedom [12–18].

velocity of the cold dark matter. This interaction is then further extended to generalised scalar-tensor theory [30]. For the dark energy modelled by vector field A_μ , a similar interaction term, $Z = A_\mu u^\mu$ was introduced in [31]. Using similar methods of [29], a generalised interacting Lagrangian with momentum transfer is studied [32], where new interaction terms were found.

Though modified theories of gravity are a promising approach to reducing the above-mentioned tensions [33]. It has been noticed that on reducing the Hubble tension either from the late-time perspective or from pre-recombination modification the value of S_8 is worsened. This is one of the challenges the modified gravity models face. Interacting dark energy is proposed to address this issue. With interacting dark energy and dark matter, it is possible to suppress the effective gravitational coupling G_{eff} of the cold dark matter [31, 32, 34, 35].

In the work, we propose an interacting dark sector, in which the interaction term between CDM and dark energy is $Z \equiv u^\mu \partial_\mu \phi$. We introduce this term into the Lagrangian by $L_{\text{int}} = G_3(\phi, X, Z) \nabla_\mu \partial^\mu \phi$. This is a novel construction, motivated from the fact that in the Horndeski theory, there exist higher derivative terms which is expected to modify the effective gravitational coupling at the level of linear perturbation. In this work, we study the effect of adding an interaction in the G_3 term of the Horndeski theory.

We derive the background and perturbation equations of motion from the action. We also derived the no-ghost and Laplacian stability conditions for tensor modes and scalar modes propagation. We also find the evolution of the matter perturbation in the quasi-static approximation. We find that the effective gravitational coupling is modified in this theory.

Since this model is theoretically viable, we used the machine learning algorithm to test its observational viability using the $H(z)$ data, and the redshift space distortion data. In particular, we use the genetic algorithm to study preliminary viability of this model, with the $H(z)$ data and $f\sigma_8$ data.

Genetic algorithm has been widely used in the context of astrophysics [36, 37] and cosmology [38–43]. It is a machine learning technique used for non-parametric reconstruction of data which is motivated by evolutionary biology. This algorithm starts with a randomly generated initial population based on the predefined grammar of basis functions such as sin, exp, log, etc., and the mathematical algebraic operations “+, −, ×, ÷”. Then the algorithm allows to generate the offspring and the fitness function is evaluated. In this context, the fitness function is the measure of how well the population describes the data, which is the measure of χ^2 . On each generation of successive populations, genetic operators like mutation and crossover are applied. This process ends once the desired criteria are reached.

Here is the basic working scheme of genetic algorithm

1. Generate an initial random population of functions $M(0)$ based on a predefined grammar.
2. Calculate the fitness for each individual in the current population $M(t)$.
3. Create the next generation $M(t + 1)$ by probabilistically choosing individuals from $M(t)$ to produce offspring through crossover and mutation, and possibly also keeping a proportion of the previous generation $M(t)$.
4. Repeat step 2 until a termination goal has been achieved.

When the next population is generated, the selection rate for the generation of the next offspring is typically 10% – 20%. The mutation rate for the generation of the next offspring is 5% ~ 10%. Mutation rate is the probability that an arbitrary part of an individual is changed. These two rates will affect the rate of convergence, and typically if we increase the rate more than what is specified, typically the algorithm will not converge. The major difference between the genetic algorithm and the standard analysis is that it does not need any model with a given number of parameters a priori. It only needs observational data; hence it can be used to test any given theory.

We can use the genetic algorithm to test a given model and see if this model can fit the observable within the error bar predicted by the genetic algorithm. We exploit this possibility to test the model we have introduced in this work. In particular, we use the $H(z)$ data and $f\sigma_8$ data compilation used in the [44]. We also use the genetic algorithm code introduced in [44].

This manuscript is arranged as follows. In the section II, we introduce the interacting model with $G_3(\phi, X, Z)$, where $X \equiv -1/2\partial_\mu \phi \partial^\mu \phi$, and $Z \equiv \partial_\mu \phi u^\mu$. Then in the section III, we derive the equations of motion for the background cosmology assuming flat-Friedmann-Lemaître-Robertson-Walker metric (FLRW) metric. In the section IV, we derive the no-ghost condition and the Laplace instability conditions for the both tensor and the scalar modes. For the tensor modes, it is trivial. In the section V, we derive the equations of motion for the linear perturbations. Subsequently, we study the evolution of the baryonic and cold dark matter over-densities in VI. Then, we introduce a concrete model in section VII and study the background dynamics and matter over-density dynamics with a concrete model. In the section VIII, we compute the $H(z)$, and $f\sigma_8$ and use genetic algorithm and test the model using $H(z)$ and $f\sigma_8$ data compilation [44] respectively. Finally, in section IX we conclude our work.

II. THE THEORY

In this section, we propose an interacting scalar field dark energy model. Usually, the interacting scalar field dark energy models are typically discussed either phenomenologically or by introducing a momentum transfer term, such as $\sqrt{-g}f(u_c^\mu \partial_\mu \phi)$, or by including conformal coupling in the Lagrangian [29, 30, 45]. In this work, we use the second proposal by introducing a momentum transfer interaction in the kinetic braiding term by adding a term $\sqrt{-g}F(u_c^\mu \nabla_\mu \phi) \nabla_\mu \nabla^\mu \phi$ into the kinetic braiding scalar-tensor theory. We name this model as G_3 interacting scalar tensor theory since the kinetic braiding term is the G_3 - term of the Horndeski gravity [20, 46]. Without loss of any generality one can consider the G_3 interaction term as two additive functions of the X and Z such as $G_3(\phi, X, Z) \nabla_\mu \nabla^\mu \phi = G(X) \nabla_\mu \nabla^\mu \phi + F(Z) \nabla_\mu \nabla^\mu \phi$. The action of the interacting scalar tensor dark energy can be written as

$$S = \int d^4x \sqrt{-g} \left[\frac{M_{\text{P}}^2}{2} R - \alpha_1 (X - V(\phi)) - G(X) \nabla_\mu \nabla^\mu \phi + F(Z) \nabla_\mu \nabla^\mu \phi \right] + S_m + S_c, \quad (2.1)$$

where g is the determinant of the metric tensor $g_{\mu\nu}$, and $X \equiv -\frac{1}{2} \partial_\mu \phi \partial^\mu \phi$. Z is the interaction term defined as

$$Z \equiv u_c^\mu \nabla_\mu \phi, \quad (2.2)$$

where u_c^μ is the four-velocity of the cold dark matter component in the universe. The coefficient α_1 is a dimensionless coefficient. The matter action for radiation and baryon is represented by S_m and given by Schutz-Sorkin action

$$S_m = - \sum_{m=b,r} \int d^4x \sqrt{-g} [\rho_m(n_m) + J_m^\mu (\partial_\mu l_m)], \quad (2.3)$$

where n_m is the number density and J_m^μ is the current density, respectively defined as

$$n_m = \sqrt{-J_m^\mu J_{m\mu} g_{\mu\nu}}, \quad (2.4)$$

and

$$J_m^\mu = n_m u_m^\mu. \quad (2.5)$$

The dark matter action is given as

$$S_c = - \int d^4x \sqrt{-g} [\rho_c(\tilde{n}) + n_c^\mu \nabla_\mu K], \quad (2.6)$$

where, ρ_c is the energy density and K is Lagrangian multiplier to impose the number density conservation.

$$\tilde{n} = -n_{c\mu} n_c^\mu. \quad (2.7)$$

This action is explored in [32] in the context of interacting vector dark energy.

III. BACKGROUND EQUATIONS OF MOTION

We consider homogeneous and isotropic flat-Friedmann-Lemaître-Robertson-Walker (FLRW) metric with scalar perturbations

$$ds^2 = -(1 + 2\alpha) dt^2 + 2\partial_i \chi d\tau dx^i + a^2 [(1 + 2\zeta) \delta_{ij} + \partial_i \partial_j E/a^2] dx^i dx^j. \quad (3.1)$$

For the fields on the matter action we define

$$J_m^\nu = \left[\frac{J_m}{a} (1 + \delta J_m), \frac{1}{a^2} \delta^{ij} \partial_j \delta j_m \right], \quad (3.2)$$

and

$$l_m = \bar{l}_m + \delta l_m. \quad (3.3)$$

We define the four-velocity of the cold dark matter component

$$u_c^\mu = \frac{n_c^\mu}{\sqrt{\bar{n}}}, \quad (3.4)$$

where

$$n_c^\mu \equiv \left[\bar{n}_0(1 + \delta n_0), \frac{1}{a^2} \delta^{il} \partial_l n_s \right], \quad (3.5)$$

then the four-velocity of the cold dark matter component automatically satisfies

$$u_c^\mu u_{\mu c} = -1, \quad (3.6)$$

and we can define the Lagrangian multiplier

$$K = K_0 + \delta K. \quad (3.7)$$

The variation with respect to the field $g_{\mu\nu}$ gives the following Friedmann equations of motion

$$3M_{\text{p}}^2 H^2 = \sum_{I=c,b,r} \rho_I + \rho_{\text{DE}}, \quad (3.8)$$

where the density of the dark energy is given by

$$\rho_{\text{DE}} \equiv -\alpha \frac{1}{2} \dot{\phi}^2 - \alpha V(\phi) + 3H \dot{\phi}^2 F_{,Z} - 3HG_{,X} \dot{\phi}^3. \quad (3.9)$$

and the second Friedmann equation can be written as

$$2M_{\text{p}}^2 \frac{\dot{H}}{a} = \sum_{I=c,b,r} (\rho_I + P_I) + \rho_{\text{DE}} + P_{\text{DE}}, \quad (3.10)$$

where the pressure of the dark energy is given by

$$P_{\text{DE}} = -\alpha \frac{1}{2} \dot{\phi}^2 + \alpha V(\phi) + F_{,Z} \dot{\phi} \ddot{\phi} - G_{,Z} \dot{\phi}^2 \ddot{\phi}. \quad (3.11)$$

The equation of state for dark energy is defined as

$$w_{\text{DE}} \equiv \frac{P_{\text{DE}}}{\rho_{\text{DE}}}. \quad (3.12)$$

Now we can also derive the equation of motion for the field ϕ

$$\begin{aligned} & \ddot{\phi} \left[\alpha + 3HF_{,Z} + \left(3H \dot{\phi} F_{,ZZ} - 6HG_{,X} \right) \dot{\phi} - 3H \dot{\phi}^3 G_{,XX} \right] + \left(-9H^2 G_{,X} - 3\dot{H} G_{,X} \right) \dot{\phi}^2 \\ & + \left(\alpha 3H + 9H^2 F_{,Z} + 3F_{,Z} \dot{H} \right) \dot{\phi} - V(\phi) = 0. \end{aligned} \quad (3.13)$$

In this section, we have derived the background equations of motion for the FLRW metric. We proceed to study the no-ghost conditions and perturbation equations of motion in the following sections.

IV. GHOST CONDITIONS

In this section, we show the no-ghost and Laplacian instability conditions for both the tensor modes and the scalar propagating modes for the model given by the action in Eq. (2.1). Since we are proposing a new interacting dark energy model, it is unavoidable to perform those analysis.

A. Tensor modes

Let us first explore the propagation of the tensor modes. Considering the tensor mode perturbation around the flat-FLRW background,

$$ds^2 = \left[-dt^2 + a(t)^2 \left(\delta_{ij} + \sum_{\lambda=+,\times} \epsilon_{ij}^\lambda h_\lambda \right) dx^i dx^j \right], \quad (4.1)$$

where we choose the metric in such a way that the tensor mode perturbations obey standard trace-less condition $\delta_{ij}\epsilon_{ij} = 0$, and divergence free gauge condition $\epsilon_{ij}^\lambda \delta^{jl} \partial_l h_\lambda = 0$. It also obeys the normalisation condition $\epsilon_{ij}^+ \epsilon_{kl}^+ \delta^{ik} \delta^{jl} = \epsilon_{ij}^\times \epsilon_{kl}^\times \delta^{ik} \delta^{jl} = 1$, with $\epsilon_{ij}^+ \epsilon_{kl}^\times \delta^{ik} \delta^{jl} = 0$. Doing the standard procedure of expanding the action Eq.(2.1) with the metric Eq.(4.1) up to second order, and substituting the background equations of motion we get the following reduced action for the tensor modes

$$S_T = \frac{M_{\text{P}}^2}{4} \sum_{\lambda=+,\times} \int d^4x a^3 \left[\dot{h}_\lambda^2 - \frac{k^2}{a^2} h_\lambda^2 \right], \quad (4.2)$$

notice that the action has been changed into Fourier space, and k is the Fourier mode. Therefore, it shows that the tensor mode propagation does not change in this theory.

B. Scalar Modes

Now let us discuss the stability conditions for scalar mode propagation. To make the calculations easy, we choose a unitary gauge, that is, we keep the fields $\delta\phi = 0$, and $E = 0$, to fix the gauge freedom. We also make the field redefinition as follows

$$\delta J_m = \frac{N_m}{a^3} \left(\frac{\rho}{n\rho,n} \delta_m - \alpha \right), \quad (4.3)$$

$$\delta n_0 = \frac{N_c}{a^3} \left(\frac{\rho_c}{2\tilde{n}\rho_{c,\tilde{n}}} \delta_c - \alpha \right), \quad (4.4)$$

then we integrate out the variables δj_m , n_s , δ_m , δ_c . Now we are remaining with the variables δl_m , δl_c , and χ , ζ and α . Varying the field χ , we get the field equation

$$\left[2M_{\text{P}}^2 H + F_{,Z} \dot{\phi}^2 - G_{,X} \dot{\phi}^3 \right] \alpha = 2M_{\text{P}}^2 \zeta - n_m \delta l_m - n_c \delta l_c. \quad (4.5)$$

We can use the above equation to replace the α field. Then, the fields χ and α are removed from the action. The remaining fields are ζ , δl_m , and δl_c , which are dynamical.

After making a few integration by part one can write the action in the form

$$\int d^3x dt a^3 \left[\dot{\mathcal{U}}^T \mathbf{K} \dot{\mathcal{U}} - \frac{k^2}{a^2} \mathcal{U}^T \mathbf{G} \mathcal{U} - \mathcal{U}^T \mathbf{M} \mathcal{U} + \mathcal{U}^T \mathbf{B} \dot{\mathcal{U}} \right], \quad (4.6)$$

where \mathbf{K} , \mathbf{G} , \mathbf{M} , and \mathbf{B} are 3×3 matrix and the vector \mathcal{U}^T is given by

$$\mathcal{U}^T \equiv (\zeta, \delta l_c, \delta l_m). \quad (4.7)$$

From the kinetic matrix, we have the following ghost conditions for the independent modes that are propagating, namely, the cold dark matter component, the matter component, consisting of relativistic particles (radiation), and non-relativistic particles (baryons), and the scalar mode

$$Q_c = (\rho_c + P_c) > 0, \quad (4.8)$$

$$Q_m = (\rho_m + P_m) > 0 \quad m = r, b, \quad (4.9)$$

$$Q_s = \frac{M_{\text{P}}^2 \dot{\phi}^2 \left[-2\alpha_1 M_{\text{P}}^2 - 6\gamma \dot{\phi}^3 F_{,Z} G_{,X} + 3\gamma^2 \dot{\phi}^2 F_{,Z}^2 - 6M_{\text{P}}^2 H \left\{ \dot{\phi} \left(\gamma F_{,ZZ} - \dot{\phi}^2 G_{,XX} - 2G_{,X} \right) + \gamma F_{,Z} \right\} + 3\dot{\phi}^4 G_{,X}^2 \right]}{\left[\dot{\phi}^2 \left(\gamma F_{,Z} - \dot{\phi} G_{,X} \right) + 2M_{\text{P}}^2 H \right]^2} > 0. \quad (4.10)$$

In the limit of no interaction we can recover the results of [46].

To find the speed of the propagation for each modes we can solve the following equation

$$\det(c_s^2 \mathbf{K} - \mathbf{G}) = 0. \quad (4.11)$$

Since the above equation is cubic in c_s^2 , we will have three solutions, which corresponds to the speed of the propagation of the three (four considering the matter to be both baryon and radiation) independent propagating modes.

The speed of propagation of the matter sector composed of radiation and baryons we get

$$c_{sm}^2 = \frac{\delta P_m}{\delta \rho_m}. \quad (4.12)$$

For the cold dark matter sector since, we assume pressure and its perturbation is vanishing, we find that

$$c_{sc}^2 = 0. \quad (4.13)$$

Finally, we have one more solution which corresponds to the propagation of the scalar mode

$$c_{s\zeta}^2 = \frac{\mathcal{A}}{\mathcal{B}}, \quad (4.14)$$

where

$$\begin{aligned} \mathcal{A} \equiv & \gamma F_{,Z} \left(3H\dot{\phi} + \ddot{\phi} \right) \left[2M_{\text{P}}^2 \dot{\phi} \left(\alpha_1 + \gamma \ddot{\phi} F_{,ZZ} + 4\gamma H F_{,Z} - 2\ddot{\phi} G_{,X} \right) + \dot{\phi}^3 \left(\gamma^2 F_{,Z}^2 - 2M_{\text{P}}^2 \ddot{\phi} G_{,XX} \right) \right. \\ & - 2\gamma \dot{\phi}^4 F_{,Z} G_{,X} + 2\gamma M_{\text{P}}^2 \ddot{\phi} F_{,Z} - 8M_{\text{P}}^2 H \dot{\phi}^2 G_{,X} + \dot{\phi}^5 G_{,X}^2 \left. \right] - \rho_c \left[2\alpha_1 M_{\text{P}}^2 + 2\gamma M_{\text{P}}^2 \ddot{\phi} F_{,ZZ} \right. \\ & \left. + 2M_{\text{P}}^2 H \left(\gamma F_{,Z} - 4\dot{\phi} G_{,X} \right) - 2\gamma \dot{\phi}^3 F_{,Z} G_{,X} + \gamma^2 \dot{\phi}^2 F_{,Z}^2 - 2M_{\text{P}}^2 \dot{\phi}^2 \ddot{\phi} G_{,XX} - 4M_{\text{P}}^2 \ddot{\phi} G_{,X} + \dot{\phi}^4 G_{,X}^2 \right], \quad (4.15) \end{aligned}$$

and

$$\begin{aligned} \mathcal{B} \equiv & \left[\gamma \dot{\phi} F_{,Z} \left(3H\dot{\phi} + \ddot{\phi} \right) - \rho_c \right] \times \\ & \left[2\alpha_1 M_{\text{P}}^2 + 6\gamma \dot{\phi}^3 F_{,Z} G_{,X} - 3\gamma^2 \dot{\phi}^2 F_{,Z}^2 + 6M_{\text{P}}^2 H \left\{ \dot{\phi} \left(\gamma F_{,ZZ} - \dot{\phi}^2 G_{,XX} - 2G_{,X} \right) + \gamma F_{,Z} \right\} - 3\dot{\phi}^4 G_{,X}^2 \right]. \quad (4.16) \end{aligned}$$

In the limit of no interaction, we recover the results of [46]. For the avoidance of the Laplacian instability we need the condition that $c_{s\zeta}^2 = \mathcal{A}/\mathcal{B} > 0$.

V. PERTURBATION EQUATIONS

Until now, we have explored the cosmological background, no-ghost and Laplacian instability conditions for the propagating scalar and tensor modes. In this section, we derive the equations of motion for the linear perturbation. Then, we study evolution of both baryonic and cold dark matter component in the quasi-static approximation limit.

We expand the action up to second order and varying the field j_m and n_s , the fields defined in Eq. (3.2) and Eq. (3.4) we get the following constraint equations respectively

$$\delta l = \rho_{,n_m} \chi + \frac{\rho_{,n_m}}{n_m} j_m, \quad (5.1)$$

$$\begin{aligned} \delta K = & \frac{a^3}{N_c} \left(-3H F_{,Z} \dot{\phi} - F_{,Z} \ddot{\phi} \right) \delta \phi + \left[\frac{2N_c}{a^3} \rho_{c,\bar{n}} + \frac{a^3}{N_c} \dot{\phi} \left(-3H F_{,Z} \dot{\phi} - F_{,Z} \ddot{\phi} \right) \right] \chi \\ & + \left[2\rho_{c,\bar{n}} + \frac{a^6}{N_c^2} \dot{\phi} \left(-3H F_{,Z} \dot{\phi} - F_{,Z} \ddot{\phi} \right) \right] n_s, \quad (5.2) \end{aligned}$$

these equations can be used to replace δl and δK and we also make another field redefinition

$$j_m = -\frac{N_m}{a^3} \frac{a}{k^2} \theta_m, \quad (5.3)$$

$$n_s = -\frac{N_{\text{cmd}}}{a^3} \frac{a}{k^2} \theta_c. \quad (5.4)$$

The second order action in Newtonian Gauge

$$\alpha = \Psi, \quad \zeta = -\Phi, \quad \chi = 0, \quad \text{and} \quad E = 0, \quad (5.5)$$

can be written as

$$S^{(2)} = \int \sqrt{-g} d^4 x a^3 \left[L_R^{(2)} + L_\phi^{(2)} + L_Z^{(2)} + L_m^{(2)} + L_c^{(2)} \right], \quad (5.6)$$

$$L_R^{(2)} \equiv M_{\text{P}}^2 \left[\frac{k^2}{a^2} \Phi (\Phi - 2\Psi) - 3 \left(H^2 \Psi^2 - \Phi^2 \dot{H} + 2H\Psi\dot{\Phi} + \dot{\Phi}^2 \right) \right], \quad (5.7)$$

$$\begin{aligned} L_\phi^{(2)} \equiv & \alpha_1 \left[\frac{k^2}{a^2} \frac{\delta\phi^2}{2} + \delta\dot{\phi} \left(3\Phi\dot{\phi} + \Psi\dot{\phi} \right) - \frac{1}{2} \delta\dot{\phi}^2 - \frac{3}{2} \Phi^2 \dot{\phi}^2 - \frac{1}{2} \Psi^2 \dot{\phi}^2 \right] - \frac{k^2}{2a^2} \delta\phi^2 \left[4H\dot{\phi}G_X + \ddot{\phi} \left(\dot{\phi}^2 G_{,XX} + 2G_X \right) \right] \\ & + \delta\dot{\phi} \left[-9H\Phi\dot{\phi}^2 G_X - 3\dot{\phi}^2 \left\{ \dot{\Phi}G_X + H\Psi \left(\dot{\phi}^2 G_{,XX} + 3G_X \right) \right\} \right] + \frac{3}{2} H\delta\dot{\phi}^2 \dot{\phi} \left(\dot{\phi}^2 G_{,XX} + 2G_X \right) \\ & + \frac{3}{2} \Phi^2 \dot{\phi}^2 G_X \left(3H\dot{\phi} - \ddot{\phi} \right) + \frac{3}{2} \Psi\dot{\phi}^3 \left[2\dot{\Phi}G_X + H\Psi \left(\dot{\phi}^2 G_{,XX} + 4G_X \right) \right] - \frac{k^2}{a^2} \delta\phi\Psi\dot{\phi}^2 G_X, \end{aligned} \quad (5.8)$$

$$\begin{aligned} L_F^{(2)} \equiv & \theta_c \left[\frac{a}{k^2} \dot{\delta}_c \dot{\phi} F_{,Z} \left(3H\dot{\phi} + \ddot{\phi} \right) - \frac{a}{k^2} 3\dot{\Phi}\dot{\phi} F_{,Z} \left(3H\dot{\phi} + \ddot{\phi} \right) \right] - \frac{3}{2} \Psi\dot{\phi}^2 \left[2\dot{\Phi}F_{,Z} + H\Psi \left(\dot{\phi} F_{,ZZ} + 3F_{,Z} \right) \right] \\ & + \delta\dot{\phi} \left[\frac{k^2}{a^2} \Psi\dot{\phi} F_{,Z} + \delta_c \left\{ \ddot{\phi}^2 F_{,ZZ} + F_{,Z} \left(3\dot{H}\dot{\phi} + \frac{d^3\phi}{dt^3} \right) + 9H^2\dot{\phi} F_{,Z} + 3H\ddot{\phi} \left(\dot{\phi} F_{,ZZ} + 2F_{,Z} \right) \right\} \right] \\ & - 3\dot{\Phi} \left\{ \ddot{\phi}^2 F_{,ZZ} + F_{,Z} \left(3\dot{H}\dot{\phi} + \frac{d^3\phi}{dt^3} \right) + 9H^2\dot{\phi} F_{,Z} + 3H\ddot{\phi} \left(\dot{\phi} F_{,ZZ} + 2F_{,Z} \right) \right\} + \frac{3}{2} \Phi^2 \dot{\phi} F_{,Z} \left(\ddot{\phi} - 3H\dot{\phi} \right) \\ & + \frac{k^2}{2a^2} \delta\phi^2 \left(\ddot{\phi} F_{,ZZ} + H F_{,Z} \right) + \delta\dot{\phi} \left[\delta_c F_{,Z} \left(3H\dot{\phi} + \ddot{\phi} \right) - 3\Phi\ddot{\phi} F_{,Z} + 3\dot{\phi} \left\{ \dot{\Phi} F_{,Z} + H\Psi \left(\dot{\phi} F_{,ZZ} + 2F_{,Z} \right) \right\} \right] \\ & - \frac{3}{2} H\delta\dot{\phi}^2 \left(\dot{\phi} F_{,ZZ} + F_{,Z} \right) + \frac{1}{2k^2} \theta_c^2 \dot{\phi} F_{,Z} \left(3H\dot{\phi} + \ddot{\phi} \right), \end{aligned} \quad (5.9)$$

$$\begin{aligned} L_m^{(2)} \equiv & -\frac{a\rho_m\theta_m\dot{\delta}_m}{k^2} + \delta_m \left(\frac{3aH\theta_m(\delta\rho_m P_m - \delta P_m \rho_m)}{k^2 \delta\rho_m} - \Psi\rho_m \right) - \frac{\theta_m(P_m + \rho_m)(\theta_m - 6a\dot{\Phi})}{2k^2} \\ & - \frac{\delta_m^2 \delta P_m \rho_m^2}{2\delta\rho_m(P_m + \rho_m)} + \frac{3}{2} \Phi^2 (P_m + \rho_m), \end{aligned} \quad (5.10)$$

$$L_c^{(2)} \equiv \theta_c \left(\frac{3a\rho_c\dot{\Phi}}{k^2} - \frac{a\rho_c\dot{\delta}_c}{k^2} \right) - \delta_c \Psi\rho_c - \frac{\rho_c\theta_c^2}{2k^2} + \frac{3}{2} \Phi^2 \rho_c. \quad (5.11)$$

A. Matter sector

On varying the fields θ_m and δ_m we get the following equations of motion

$$E_{\theta_m} \equiv \dot{\delta}_m + 3H \left(\frac{\delta P_m}{\delta\rho_m} - \frac{P_m}{\rho_m} \right) \delta_m + \left(1 + \frac{P_m}{\rho_m} \right) \frac{\theta_m}{a} - 3 \left(1 + \frac{P_m}{\rho_m} \right) \dot{\Phi}, \quad (5.12)$$

$$E_{\delta_m} \equiv \dot{\theta}_m + H \left(1 - 3 \frac{\delta P_m}{\delta\rho_m} \right) \theta_m - \frac{k^2}{a} \left(\frac{\delta P_m / \delta\rho_m}{1 + P_m / \rho_m} \right) \delta_m - \frac{k^2}{a} \Psi + k^2 \sigma_m. \quad (5.13)$$

These equations are the equations of motion of the standard matter fluids in the system we are considering, in particular, radiation and baryon. For the baryon, we have $P_b = 0$ and $\delta P_b = 0$. We can add an effective shear term to the matter action $S_{\text{shear}}^{(2)} = \int dt d^3 x a^4 \sigma_m [\delta\rho_m + (\rho_m + P_m)\zeta]$ [15], such that we get the equations of motion with the shear term.

B. Dark matter sector

Now we find the following equations of motion for the dark matter fluid. Here, we can see the implications of the interaction we have considered. The evolution of cold dark matter over-density is

$$E_{\theta_c} \equiv \dot{\delta}_c + \frac{\theta_c}{a} - 3\dot{\Phi} = 0, \quad (5.14)$$

and the evolution of the velocity potential is

$$\begin{aligned} E_{\delta_c} \equiv & \frac{k^2 \delta \dot{\phi} F_{,Z} (3H\dot{\phi} + \ddot{\phi})}{a [\rho_c - \dot{\phi} F_{,Z} (3H\dot{\phi} + \ddot{\phi})]} + \frac{k^2 \delta \phi \left[\ddot{\phi}^2 F_{,ZZ} + F_{,Z} (3\dot{H}\dot{\phi} + \frac{d^3\phi}{dt^3}) + 9H^2 \dot{\phi} F_{,Z} + 3H\ddot{\phi} (\dot{\phi} F_{,ZZ} + 2F_{,Z}) \right]}{a [\rho_c - \dot{\phi} F_{,Z} (3H\dot{\phi} + \ddot{\phi})]} \\ & - \frac{\theta_c \left[\dot{\phi} \ddot{\phi}^2 F_{,ZZ} + F_{,Z} (3\dot{H}\dot{\phi}^2 + \ddot{\phi}^2 + \frac{d^3\phi}{dt^3} \dot{\phi}) + 12H^2 \dot{\phi}^2 F_{,Z} + H\dot{\phi} \ddot{\phi} (3\dot{\phi} F_{,ZZ} + 10F_{,Z}) - H\rho_c \right]}{\rho_c - \dot{\phi} F_{,Z} (3H\dot{\phi} + \ddot{\phi})} \\ & - \frac{k^2 \psi \rho_c}{a [\rho_c - \dot{\phi} F_{,Z} (3H\dot{\phi} + \ddot{\phi})]} + \dot{\theta}_c = 0. \end{aligned} \quad (5.15)$$

C. Gravity Sector

Here are the equations of motion for the gravity sector, including the scalar field equation of motion. The Hamiltonian constraint equation is

$$\begin{aligned} E_\alpha \equiv & - \sum_{I=c,r,b} \delta_I \rho_I + \left(3H\dot{\phi}^2 F_{,ZZ} + 6H\dot{\phi} F_{,Z} + \alpha_1 \dot{\phi} - 9H\dot{\phi}^2 G_{,X} - 3H\dot{\phi}^4 G_{,XX} \right) \delta\dot{\phi} + \left[\frac{k^2}{a^2} (\dot{\phi} G_{,Z} - \dot{\phi}^2 G_{,X}) \right] \delta\phi \\ & + \left(-3H\dot{\phi}^3 F_{,ZZ} - 9H\dot{\phi}^2 F_{,Z} - \alpha_1 \dot{\phi}^2 - 6M_{\text{P}}^2 H^2 + 12H\dot{\phi}^3 G_{,X} + 3H\dot{\phi}^5 G_{,XX} \right) \Psi - \frac{k^2}{a^2} 2k^2 M_{\text{P}}^2 \Phi \\ & + \left(-3\dot{\phi}^2 F_{,Z} + 3G_{,X} \dot{\phi}^3 - 6M_{\text{P}}^2 H \right) \dot{\Phi} = 0. \end{aligned} \quad (5.16)$$

The momentum constraint equation is

$$\begin{aligned} E_\chi \equiv & - \frac{k^2}{a^2} (-\dot{\phi} F_{,Z} + \dot{\phi}^2 G_{,X}) \delta\dot{\phi} + \frac{k^2}{a^2} (\dot{\phi} - 3HG_X \dot{\phi}^2 - \ddot{\phi} F_{,Z}) \delta\phi + \frac{k^2}{a^2} (2M_{\text{P}}^2 H + \dot{\phi}^2 F_{,Z} - \dot{\phi}^3 G_{,X}) \Psi + \frac{k^2}{a^2} 2M_{\text{P}}^2 \dot{\Phi} \\ & + \frac{\theta_c}{a} \left[3H\dot{\phi}^2 F_{,Z} + \dot{\phi} \ddot{\phi} F_{,Z} - (\rho_c + P_c) \right] - \sum_{I=b,r} \frac{\theta_I}{a} (\rho_I + P_I) = 0. \end{aligned} \quad (5.17)$$

The equation of motion for the field ζ is

$$\begin{aligned} E_\zeta \equiv & \Psi \left[\frac{k^2}{3a^2} + \frac{\alpha \dot{\phi}^2}{2M_{\text{P}}^2} - \frac{\dot{\phi}^2 \ddot{\phi} F_{,ZZ}}{2M_{\text{P}}^2} - \frac{3\dot{\phi} \ddot{\phi} F_{,Z}}{2M_{\text{P}}^2} + \frac{\dot{\phi}^4 \ddot{\phi} G_{,XX}}{2M_{\text{P}}^2} + \frac{2\dot{\phi}^2 \ddot{\phi} G_{,X}}{M_{\text{P}}^2} - 2\dot{H} - 3H^2 \right] - \frac{k^2}{3a^2} \Phi - \alpha_1 \frac{\dot{\phi}}{2M_{\text{P}}^2} \delta\dot{\phi} \\ & + \sum_{I=r,b,c} \frac{\delta P_I}{2M_{\text{P}}^2} + \delta\ddot{\phi} \left[\frac{\dot{\phi} F_{,Z}}{2M_{\text{P}}^2} - \frac{\dot{\phi}^2 G_{,X}}{2M_{\text{P}}^2} \right] + \frac{\dot{\phi} \ddot{\phi} F_{,ZZ}}{2M_{\text{P}}^2} \delta\dot{\phi} + \frac{\ddot{\phi} F_{,Z}}{2M_{\text{P}}^2} \delta\phi - \frac{\dot{\phi}^3 \ddot{\phi} G_{,XX}}{2M_{\text{P}}^2} \delta\dot{\phi} - \frac{\dot{\phi} \ddot{\phi} G_{,X}}{M_{\text{P}}^2} \delta\dot{\phi} \\ & + \dot{\Psi} \left[-\frac{\dot{\phi}^2 F_{,Z}}{2M_{\text{P}}^2} + \frac{\dot{\phi}^3 G_{,X}}{2M_{\text{P}}^2} - H \right] - 3H\dot{\Phi} - \ddot{\Phi} = 0. \end{aligned} \quad (5.18)$$

The shear equation of motion is given by

$$E_{\text{shear}} \equiv M_{\text{P}}^2 k^2 (\Psi - \Phi) + \frac{3}{2} a^2 (P_r + \rho_r) \sigma_r = 0. \quad (5.19)$$

Finally, the equation of motion for the scalar mode is given by

$$\begin{aligned}
E_{\delta\phi} \equiv & \frac{k^2}{a^2} \left[-G_{,XX} \ddot{\phi} \dot{\phi}^2 + \alpha_1 + H \left(F_{,Z} - 4G_{,X} \dot{\phi} \right) - 2G_{,X} \ddot{\phi} + F_{,ZZ} \ddot{\phi} \right] \delta\phi + \delta\ddot{\phi} \left[\alpha_1 + 3H \left\{ F_{,Z} + \dot{\phi} \left(-G_{,XX} \dot{\phi}^2 - 2G_{,X} + F_{,ZZ} \right) \right\} \right] \\
& + \dot{\Psi} \dot{\phi} \left[H \left\{ 3\dot{\phi} \left(G_{,XX} \dot{\phi}^2 + 3G_{,X} - F_{,ZZ} \right) - 6F_{,Z} \right\} - \alpha_1 \right] + 3\dot{\phi} \left(G_{,X} \dot{\phi} - F_{,Z} \right) \ddot{\Phi} + \left[F_{,Z} \left(3H\dot{\phi} + \ddot{\phi} \right) / a \right] \theta_c \\
& - 3\dot{\Phi} \left[-G_{,XX} \ddot{\phi} \dot{\phi}^3 - 6HG_{,X} \dot{\phi}^2 + \left(\alpha_1 + 6HF_{,Z} - 2G_{,X} \ddot{\phi} + F_{,ZZ} \ddot{\phi} \right) \dot{\phi} + F_{,Z} \ddot{\phi} \right] \\
& - 3\Phi \left[9\dot{\phi} \left(F_{,Z} - G_{,X} \dot{\phi} \right) H^2 + 3 \left\{ -G_{,XX} \ddot{\phi} \dot{\phi}^3 + \left(\alpha_1 - 2G_{,X} \ddot{\phi} + F_{,ZZ} \ddot{\phi} \right) \dot{\phi} + F_{,Z} \ddot{\phi} \right\} H - 3G_{,X} \dot{H} \dot{\phi}^2 + 3F_{,Z} \dot{H} \dot{\phi} + \alpha_1 \ddot{\phi} \right] \\
& + 3\delta\dot{\phi} \left[3 \left\{ F_{,Z} + \dot{\phi} \left(-G_{,XX} \dot{\phi}^2 - 2G_{,X} + F_{,ZZ} \right) \right\} H^2 + \left(-\ddot{\phi} G_{,XX} \dot{\phi}^4 - 5G_{,XX} \ddot{\phi} \dot{\phi}^2 + \ddot{\phi} F_{,ZZ} \dot{\phi} \right. \right. \\
& \left. \left. + \alpha_1 - 2G_{,X} \ddot{\phi} + 2F_{,ZZ} \ddot{\phi} \right) H + \dot{H} \left\{ F_{,Z} + \dot{\phi} \left(-G_{,XX} \dot{\phi}^2 - 2G_{,X} + F_{,ZZ} \right) \right\} \right] \\
& + \Psi \left[3\dot{H} G_{,XX} \dot{\phi}^4 + 9G_{,X} \dot{H} \dot{\phi}^2 - 3\dot{H} F_{,ZZ} \dot{\phi}^2 - 6F_{,Z} \dot{H} \dot{\phi} + k^2/a^2 \left(F_{,Z} - G_{,X} \dot{\phi} \right) \dot{\phi} \right. \\
& \left. - 9H^2 \left\{ 2F_{,Z} + \dot{\phi} \left(-G_{,XX} \dot{\phi}^2 - 3G_{,X} + F_{,ZZ} \right) \right\} \dot{\phi} - \alpha_1 \ddot{\phi} - 3H \left\{ -\ddot{\phi} G_{,XX} \dot{\phi}^5 - 7G_{,XX} \ddot{\phi} \dot{\phi}^3 + \ddot{\phi} F_{,ZZ} \dot{\phi}^2 \right. \right. \\
& \left. \left. + \left(\alpha - 6G_{,X} \ddot{\phi} + 4F_{,ZZ} \ddot{\phi} \right) \dot{\phi} + 2F_{,Z} \ddot{\phi} \right\} \right] = 0. \tag{5.20}
\end{aligned}$$

VI. QUASI-STATIC APPROXIMATION AND EFFECTIVE GRAVITATIONAL CONSTANTS

In this section, we study the evolution of the baryonic and cold dark matter over-densities using the quasi-static approximation (QSA) limit. Let us start from the matter equation

$$E_{\theta_b} \equiv \dot{\delta}_b + \frac{\theta_b}{a} = 0, \tag{6.1}$$

$$E_{\delta_b} \equiv \dot{\theta}_b + H\theta_b - \frac{k^2}{a} \Psi = 0. \tag{6.2}$$

where we have considered that the contribution of matter is for the baryon, i.e. $P_b = 0$. Then we have

$$\ddot{\delta}_b + 2H\dot{\delta}_b + \frac{k^2}{a^2} \Psi = 0. \tag{6.3}$$

Following the same procedure for the dark matter sector we have

$$E_{\theta_c} \equiv \dot{\delta}_c + \frac{\theta_c}{a} = 0, \tag{6.4}$$

and the equation of motion for the velocity potential, Eq. (5.15) remains the same in the quasi-static approximation limit. Taking the time derivative of the Eq. (6.4) and substituting the $\dot{\theta}_c$ and θ_c , with Eq. (5.15), resulting in

$$E_{\delta}(\ddot{\delta}_c, \dot{\delta}_c, \Phi, \delta\dot{\phi}, \delta\phi), \tag{6.5}$$

where, we have used $\Phi = \Psi$ from the shear equation Eq. (5.19), since $\sigma = 0$ for baryons.

Now we need to find the solution for Φ and $\delta\phi$ in the QSA limit. On taking the QSA limit of the Eq. (5.16), we get

$$E_{\alpha}^{\text{QSA}} \equiv -\rho_b \delta_b - \rho_c \delta_c + \frac{k^2}{a^2} \left[-2M_{\text{P}}^2 \Phi + \delta\phi \left(\dot{\phi} F_{3,Z} + \dot{\phi}^2 G_{,X} \right) \right] \simeq 0, \tag{6.6}$$

Notice that in the quasi-static approximation, the momentum equation remains the same. Now taking the time derivative of the Eq. (6.6), and from the linear combination of Eq. (5.17), and using Eq. (6.6), we arrive at

$$\frac{k^2}{a^2} A \delta\phi \simeq 2M_{\text{P}}^2 \dot{\delta}_c F_{,Z} \left(3H\dot{\phi} + \ddot{\phi} \right) + \delta_c \rho_c \dot{\phi} \left(F_{,Z} - \dot{\phi} G_{,X} \right) + \delta_b \rho_b \dot{\phi} \left(F_{,Z} - \dot{\phi} G_{,X} \right), \tag{6.7}$$

where A is given by

$$\begin{aligned}
A \equiv & \alpha_1 2M_{\text{P}}^2 + 2M_{\text{P}}^2 \ddot{\phi} F_{,ZZ} - 2\dot{\phi}^3 F_{,Z} G_{,X} + \dot{\phi}^2 F_{,Z}^2 + 2M_{\text{P}}^2 H F_{,Z} - 2M_{\text{P}}^2 \dot{\phi}^2 \ddot{\phi} G_{,XX} - 8M_{\text{P}}^2 H \dot{\phi} G_{,X} \\
& - 4M_{\text{P}}^2 \ddot{\phi} G_{,X} + \dot{\phi}^4 G_{,X}^2. \tag{6.8}
\end{aligned}$$

Now we have solution for the $\delta\phi$, given by Eq. (6.7) Ψ (by solving Eq. (6.6), and substituting $\delta\phi$).

On inserting the solution for Ψ and $\delta\phi$ we can write the second-order equation for the baryonic over-density and the cold dark matter over-density, we get

$$\ddot{\delta}_b + 2H\dot{\delta}_b + \Gamma_{bc}\dot{\delta}_c - \frac{3}{2}\frac{H^2}{G}a^2(G_{bb}\Omega_b\delta_b + G_{bc}\Omega_c\delta_c) = 0, \quad (6.9)$$

and

$$\ddot{\delta}_c + 2H\Gamma_{cc}\dot{\delta}_c + \Gamma_{cb}\dot{\delta}_b - \frac{3}{2}\frac{H^2}{G}a^2(G_{cb}\Omega_b\delta_b + G_{cc}\Omega_c\delta_c) = 0, \quad (6.10)$$

where

$$\Gamma_{bc} \equiv \frac{\dot{\phi}F_{,Z}(3H\dot{\phi} + \ddot{\phi})(F_{,Z} - \dot{\phi}G_{,X})}{A}, \quad (6.11)$$

and

$$G_{bb} = G_{bc} = \frac{2M_{\text{P}}^2 \left[\alpha_1 + \gamma\ddot{\phi}F_{,ZZ} + H(\gamma F_{,Z} - 4\dot{\phi}G_{,X}) + \dot{\phi}^2\ddot{\phi}(-G_{,XX}) - 2\ddot{\phi}G_{,X} \right]}{A}. \quad (6.12)$$

The expression for Γ_{cc} , Γ_{cb} , G_{cb} and G_{cc} is given in Appendix A.

VII. CONCRETE MODEL

Until now, we considered the model to be completely general. We have already found the background equations of motion, no-ghost condition, Laplace instability conditions, and the perturbed equations of motion. Now we introduce a concrete model

$$G(X) = \beta\frac{X}{M^3}, \quad F(Z) = \gamma\frac{Z^2}{M^3}. \quad (7.1)$$

This model has a tracking behaviour $\dot{\phi}H = \text{constant}$ [47]. In the following subsections, we study the background dynamics, no-ghost conditions and evolution of the matter over-densities with the concrete model.

A. Background and Ghost conditions

1. Background dynamics

We introduce the following redefinition, which has been introduced in [47]

$$r_1 \equiv \frac{H_{\text{dS}}\dot{\phi}_{\text{dS}}}{H\dot{\phi}}, \quad r_2 \equiv \left(\frac{\dot{\phi}}{\dot{\phi}_{\text{dS}}} \right)^4 \frac{1}{r_1}, \quad (7.2)$$

where H_{dS} and $\dot{\phi}_{\text{dS}}$ is the value of Hubble expansion and the value of $\dot{\phi}$ at the de Sitter solution respectively. Since at de Sitter, all the matter content will be absent, we can keep $\gamma = 0$ at the de Sitter.

Now we can find that

$$\frac{r'_1}{r_1} = -\frac{\dot{H}}{H^2} - \frac{\ddot{\phi}}{H\dot{\phi}}, \quad \text{and} \quad \frac{r'_2}{r_2} = -\frac{r'_1}{r_1} - \frac{4\ddot{\phi}}{H\dot{\phi}}, \quad (7.3)$$

where the prime denotes the derivative with respect to the variable $\mathcal{N} = \ln(a)$ and over dot denotes the derivative with respect to time. We can use Eq. (3.10) and Eq. (3.13) to substitute $\ddot{\phi}$ and \dot{H} .

Now considering the Eq. (3.8) and Eq. (3.10) at de Sitter, i.e. all the matter content vanishing including the interaction term and $\ddot{\phi} = 0$, $\dot{H} = 0$. Then we can find that

$$\alpha_1 = \frac{6}{x_{\text{dS}}^2}, \quad \text{and} \quad \beta = \frac{2}{x_{\text{dS}}}, \quad \text{where} \quad x_{\text{dS}} = \frac{\dot{\phi}_{\text{dS}}}{M_{\text{P}}H_{\text{dS}}}. \quad (7.4)$$

We also introduce the density variables

$$\Omega_i \equiv \frac{\rho_i}{3M_{\text{P}}^2 H^2}. \quad (7.5)$$

We can write dark energy energy density as

$$\Omega_{\text{DE}} = -\frac{1}{6}\alpha_1 x_{\text{dS}}^2 r_1^3 r_2 - \beta x_{\text{dS}}^3 r_1^2 r_2 - 2\gamma x_{\text{dS}} r_1^2 r_2, \quad (7.6)$$

where we have also used the relation

$$M^3 \equiv H_{\text{dS}}^2 M_{\text{P}}. \quad (7.7)$$

We also use the Friedmann constrain to replace Ω_b

$$\Omega_b = 1 - \Omega_r - \Omega_c - \Omega_{\text{DE}}. \quad (7.8)$$

After choosing the concrete model and making the field redefinitions to new variables, we can rewire the background equations of motion in terms of new variables. The evolution of the variable r_1 is given by

$$\frac{r_1'}{r_1} - \frac{(r_1 + \gamma x_{\text{dS}}^3 - 1) (6 (\gamma x_{\text{dS}}^3 - 1) r_1^2 r_2 + 3r_1^3 r_2 - \Omega_r - 9)}{2 \left((\gamma x_{\text{dS}}^3 - 1)^2 r_1^2 r_2 - r_1 - 2\gamma x_{\text{dS}}^3 + 2 \right)} = 0, \quad (7.9)$$

the evolution of r_2 is given by

$$\frac{r_1'}{r_1} + \frac{r_2'}{r_2} - \frac{2 (3 (\gamma x_{\text{dS}}^3 - 1) r_1^3 r_2 + 6r_1 + (1 - \gamma x_{\text{dS}}^3) \Omega_r + 3\gamma x_{\text{dS}}^3 - 3)}{(\gamma x_{\text{dS}}^3 - 1)^2 r_1^2 r_2 - r_1 - 2\gamma x_{\text{dS}}^3 + 2} = 0. \quad (7.10)$$

The evolution of the variable Ω_r is,

$$4 \frac{\Omega_r'}{\Omega_r} - 10 \frac{r_1'}{r_1} - 2 \frac{r_2'}{r_2} + 16 = 0. \quad (7.11)$$

Finally, we can also find the differential equation for Ω_c as

$$\frac{\Omega_c'}{\Omega_c} - \frac{5r_1'}{2r_1} - \frac{r_2'}{2r_2} + 3 = 0. \quad (7.12)$$

We solve the coupled differential equations for the variables r_1 , r_2 , Ω_r , and Ω_c numerically giving the following initial conditions $r_1 = 1$, $r_2 = 1.2 \times 10^{-58}$, $\Omega_r = 0.99998$, $\Omega_c = 1.85 \times 10^{-5}$ and $\Omega_b = 3.7 \times 10^{-6}$ at $\mathcal{N} = \ln(a) = -19$. The resulting evolution is presented in the figure 1.

The figure 1 shows that, in this model, the behaviour of the composition of our universe at the background level behaves as expected. The new contribution in this model is the interaction Z in the G_3 term in the Lagrangian, which is proportional to γ , where we choose $\gamma = 0.01$.

2. Stability conditions

In this part, we show the behaviour of the no-ghost condition and the square of the speed of propagation for the scalar mode. After choosing the concrete model and making the field redefinition, the no-ghost condition for the scalar mode becomes

$$Q_s/M_{\text{P}}^2 = \frac{3r_1^2 r_2 (r_1 + 2\gamma x_{\text{dS}} - 2) [(\gamma x_{\text{dS}} - 1)^2 r_2 (r_1 + 2\gamma x_{\text{dS}} - 2) - 1]}{[2(\gamma x_{\text{dS}} - 1)^2 r_1 r_2 + (\gamma x_{\text{dS}} - 1) r_1^2 r_2 - 1]^2} > 0, \quad (7.13)$$

where $\gamma x_{\text{dS}} \equiv \gamma x_{\text{dS}}^3$.

The behaviours of the Q_s/M_{P}^2 , and the $c_{s\zeta}^2$ is given in the figure 2. We have used same initial values for the variables r_1 , r_2 , Ω_r , and Ω_c as for the figure 1.

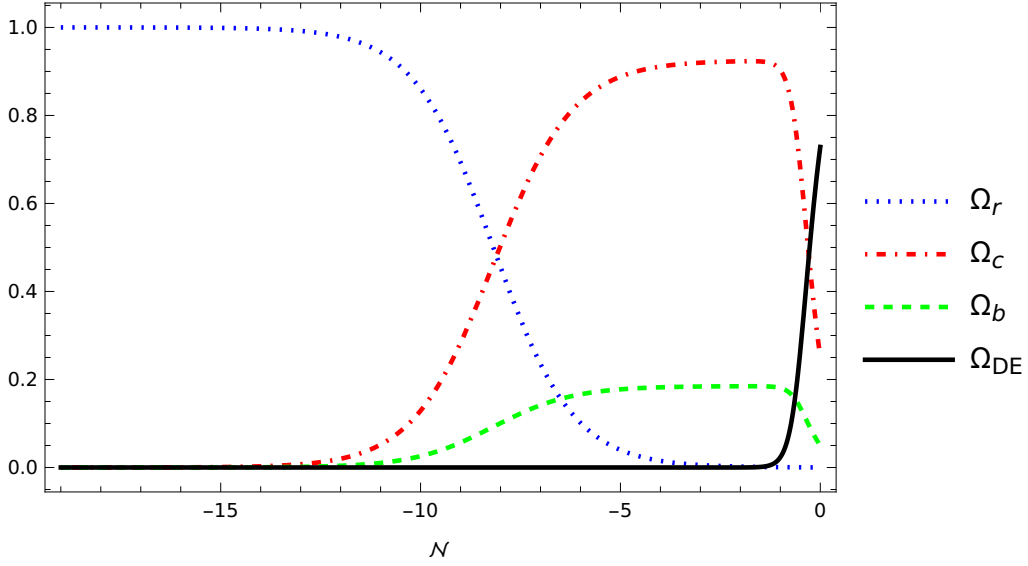


FIG. 1. Evolution of Ω_{DE} , Ω_r , Ω_c , Ω_b . This plot is generated by solving the coupled background equations for r_1 , r_2 , and Ω_r as given in Eq. (7.9), Eq. (7.10), Eq. (7.11). The differential equation for Ω_c is given in Eq. (7.12). Ω_{DE} is given in terms of the variable r_1 and r_2 in Eq. (7.6). We also have chosen $\gamma = 0.01$.

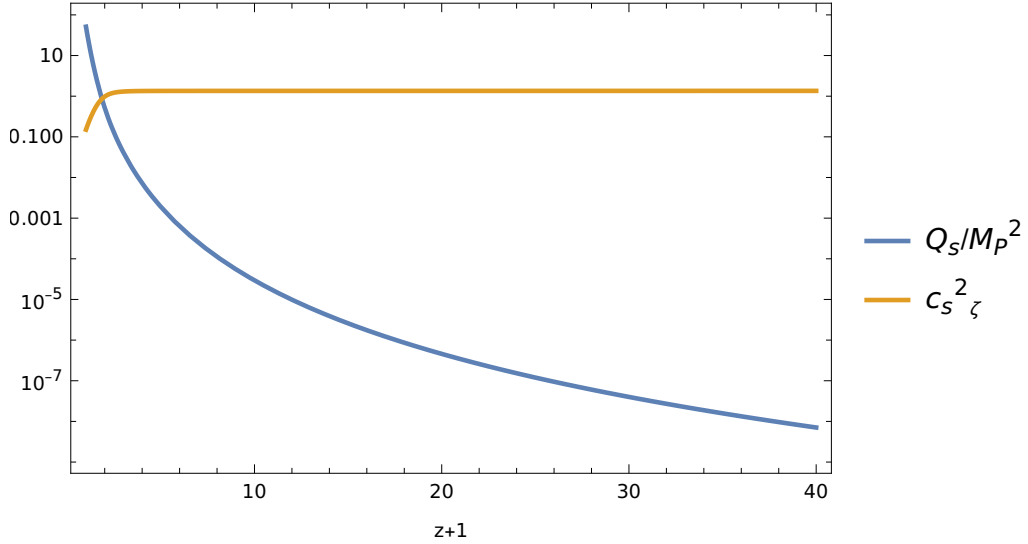


FIG. 2. Behaviour of the Q_s/M_P^2 and $c_s^2 \zeta$. We have used the same initial conditions to solve the background differential equations with $\gamma = 0.01$, and $x_{\text{as}} = 1$.

B. Dynamics of matter over-densities

Now we study the evolution of the baryonic and cold dark matter over-densities. We solve numerically the Eq. (6.9) and Eq. (6.10), using the concrete model Eq. (7.1) we have introduced in this section. The evolution is plotted in the figure 3. We used the initial condition $\delta'_{m=c,b} = \delta_{m=c,b} = 0.017$ at the redshift $z = 39.45$. We also plot the total matter over-density given by

$$\delta_{\text{M}} = \frac{\Omega_b \delta_b}{(\Omega_b + \Omega_c)} + \frac{\Omega_c \delta_c}{(\Omega_b + \Omega_c)}. \quad (7.14)$$

We can clearly see in the figure 3 that there is an enhanced growth to the cold dark matter component, with respect to the baryonic component, hence the total matter component also shows an enhanced growth. We will see in the next section the effect of this modification in the redshift space distortion observable.

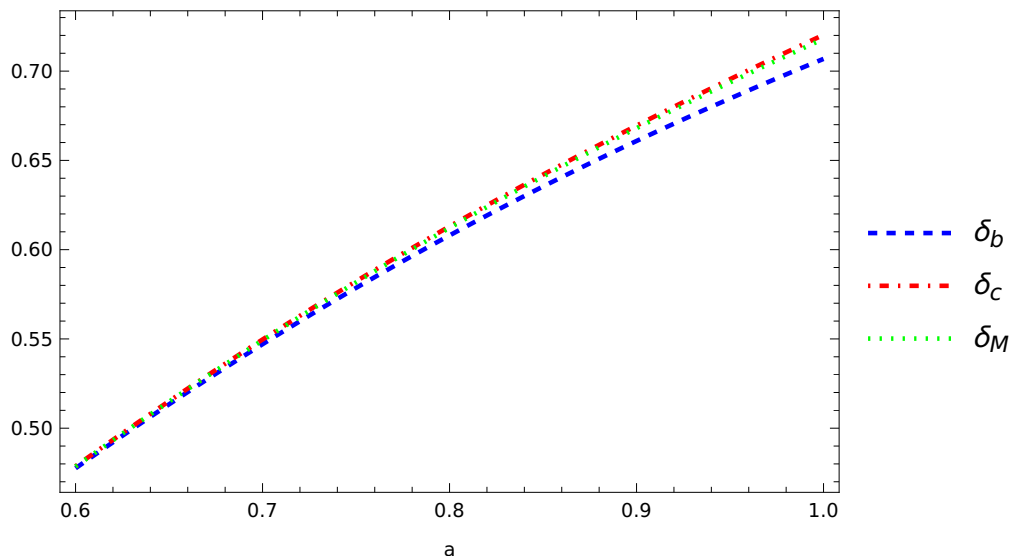


FIG. 3. Evolution of the fields δ_c (dot dashed red), δ_b (dashed blue), and the total matter over-density δ_M (dotted red).

VIII. TESTING THE MODEL USING GENETIC ALGORITHM

Until now, we have computed the background equations of motion, ghost conditions, perturbation equations as well as the equations of motion for the baryon and the cold dark matter over-densities. Also, we analysed their evolution along the redshift after introducing a concrete model for the free functions. In this section, we move on to use the genetic algorithm to make an initial test of the theory we introduced.

A. $H(z)$ data

In this subsection, we study the compatibility of background dynamics with genetic algorithm, using the cosmological data. In particular, we use $H(z)$ data compilations used in [44]. These data are given in table I, which consists of 39 data points. Now we use the genetic algorithm code provided in the [44], to predict the $H(z)$ curve using the data provided. We use the set of orthogonal functions, also known as grammar, to be x and x^x . We have chosen the crossover rate to be 0.75 and the mutation rate to be 0.25, with 1500 generations. If the χ^2 is not improved for a few hundred generations the algorithm is stopped. The resulting curve is plotted in the figure 4.

The function $H(z)$ predicted by the genetic algorithm is

$$H(z)^{GA} = H_{\text{marg}}^{GA} 67.5443 \sqrt{z(0.453104z + 1.01544)^2 + 1} \quad (8.1)$$

with the $\chi_{\text{min}}^2 = 1066.87$, and H_{marg}^{GA} is the marginalised value of the Hubble function today $H_{\text{marg}}^{GA} = 67.54$.

A methodology of error estimation in the genetic algorithm is developed in [48] using the path integral technique. We use the same algorithm to estimate the error up to 1σ which is shown in the figure. We also over plot the $H(z)$ function from the background dynamics of the model we have considered, and we choose $H_{\text{dS}} = 67$. It is clear from the figure 4 that, $H(z)$ function is well inside the 1σ region. In other words, the genetic algorithm validates the model at the level of background dynamics.

B. RSD data

We have seen that the model we have introduced can modify the effect of gravitational coupling and hence can modify the evolution of the baryon and cold dark matter over-densities. We solved numerically the evolution of these over-densities using the concrete model we have introduced in the previous section. After solving the equations, we can compute $f\sigma_8$ for this model. Then we can use a genetic algorithm to test if this model is viable at the linear perturbation level. We will find that, since this model shows an enhanced behaviour in the growth of the structures

Redshift (z)	$H(z)$	1σ	Ref.
0.09	69	12	[49]
0.17	83	8	[49]
0.27	77	14	[49]
0.40	95	17	[49]
0.48	97	62	[49]
0.88	90	40	[49]
0.90	117	23	[49]
1.30	168	17	[49]
1.43	177	18	[49]
1.53	140	14	[49]
1.75	202	40	[49]
0.44	82.6	7.8	[50]
0.60	87.9	6.1	[50]
0.73	97.3	7.0	[50]
0.179	75	4	[51]
0.199	75	5	[51]
0.352	83	14	[51]
0.593	104	13	[51]
0.68	92	8	[51]
0.781	105	12	[51]
0.875	125	17	[51]
1.037	154	20	[51]
0.35	82.7	8.4	[52]
0.07	69.0	19.6	[53]
0.12	68.6	26.2	[53]
0.20	72.9	29.6	[53]
0.28	88.8	36.6	[53]
0.57	96.8	3.4	[54]
2.34	222.0	7.0	[55]
1.363	160.0	33.6	[56]
1.965	186.5	50.4	[56]
0.3802	83.0	13.5	[57]
0.4004	77.0	10.2	[57]
0.4247	87.1	11.2	[57]
0.4497	92.8	12.9	[57]
0.4783	80.9	9.0	[57]
0.47	89	50	[58]
0.75	98.8	33.6	[59]
0.80	113.1	20.73	[60]

TABLE I. This table shows the $H(z)$ data compilations and the corresponding 1σ error bars from various observations. We have also given the corresponding references.

the value of $f\sigma_8$ in the redshift close to today lies outside the 1σ error bar determined by the genetic algorithm. Even though, this model shows less preference with the genetic algorithm, we have not tried complete parameter estimation to find the value of the new parameter γ corresponding to the new interaction we have introduced.

The redshift space distortion observable is given by

$$f\sigma_8 = f(a)\sigma(a) = \frac{\sigma_{8,0}}{\delta_{m,0}} a \frac{d\delta_m}{da}, \quad (8.2)$$

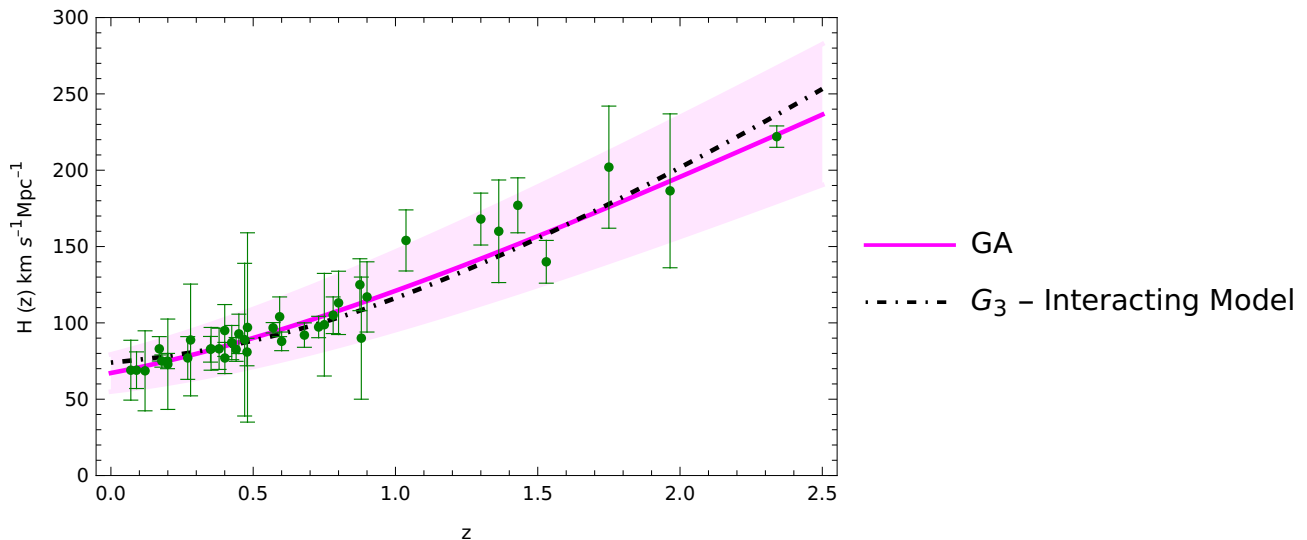


FIG. 4. This plot shows the $H(z)$ curve predicted by the genetic algorithm (magenta line), using the data points given in the figure (green points) with error bars. The light shaded region is the 1σ error predicted by the algorithm. The dotted dashed line shows the $H(z)$ given by the G_3 interacting model.

where

$$f(a) = \frac{d \ln(\delta_m)}{da}, \quad \sigma(a) = \sigma_{8,0} \frac{\delta_m}{\delta_{m,0}}. \quad (8.3)$$

$\delta_{m,0}$ is the value of δ_m today. The δ_m we consider from this model is for the total matter content given as in Eq. (7.14), and we choose $\sigma_{8,0} = 0.8$ and $\delta_{m,0} = 0.718064$.

We consider the redshift space distortion data that as been compiled in the [44], the data is given in the table II. We use these data as the input to the genetic algorithm to predict $f\sigma_8$ curve model independently [44, 61]. We use the same error estimation method developed in [48] to estimate the error up to 1σ .

The set of orthogonal functions (grammar) that we have used in our GA analysis are x and x^x . We have chosen the crossover rate and the mutation rate as 0.75 and 0.25 respectively, with 1500 generations. The algorithm will be terminated once the χ^2 does not improve for a few hundred generations. The resulting curve is given in the figure 5. We also plotted the $f\sigma_8$ predicted by the model choosing one particular value of $\gamma = 0.01$, which is the new parameter in the model. It is clear that the value of $f\sigma_8$ in the redshift close to today deviates from the 1σ predicted by GA, using the RSD data compilation as given in the table II.

The best function concluded by the GA with the given RSD data is

$$f\sigma_8^{(GA)}(a) = a - a^4 \left(-0.988584 + 0.206888a^{2.90671} + 0.0165351a^{4.5531} - 0.122587(0.417286^{0.417286a} \times a^{0.417286a})^{5.97559} \right)^2, \quad (8.4)$$

with the $\chi_{\min}^2 = -17.173$.

It is true that from the GA analysis, the model is less preferred with the RSD data set. This enhancement in the growth can be understood from the evolution of the matter over-densities, since there is an enhanced growth of the over-densities. This is due to the fact that the ratio of effective gravitational coupling to G_N grows above unity in the dark sector domination as shown in the appendix B.

In fact, we have only analysed this model with a particular value of the new parameter. It would be interesting to know if there are other values for the γ , which can fit with the data. To study this we need to do a complete parameter estimation using MCMC methods. This will also allow us to confront the model with other data sets like cosmic microwave background and other large scale structure data, which will be done in a future work.

IX. CONCLUSION

In this manuscript, we have attempted to develop a new interacting scalar dark energy, with only momentum transfer, by adding the term $G_3(X, Z)\nabla_\mu\nabla^\mu\phi = G(X)\nabla_\mu\nabla^\mu\phi + F(Z)\nabla_\mu\nabla^\mu\phi$, where $Z = u^\mu\nabla_\mu\phi$. We started the

Redshift (z)	$f\sigma_8$	1σ	$\Omega_{m,0}$	Ref.
0.17	0.510	0.060	0.3	[62]
0.02	0.314	0.048	0.266	[63, 64]
0.02	0.398	0.065	0.3	[64, 65]
0.44	0.413	0.080	0.27	[50]
0.60	0.390	0.063	0.27	[50]
0.73	0.437	0.072	0.27	[50]
0.18	0.360	0.090	0.27	[66]
0.38	0.440	0.060	0.27	[66]
1.40	0.482	0.116	0.27	[67]
0.02	0.428	0.0465	0.3	[68]
0.60	0.550	0.120	0.3	[69]
0.86	0.400	0.110	0.3	[69]
0.03	0.404	0.0815	0.312	[70]
0.013	0.46	0.060	0.315	[71]
0.15	0.530	0.160	0.31	[72]
0.38	0.500	0.047	0.31	[72]
0.51	0.455	0.039	0.31	[72]
0.70	0.448	0.043	0.31	[72]
0.85	0.315	0.095	0.31	[72]
1.48	0.462	0.045	0.31	[72]

TABLE II. This table shows the value of $f\sigma_8$, corresponding 1σ error bar, which is compiled in [44]. The table also gives the corresponding value of $\Omega_{m,0}$ used, which is the assumption of the fiducial background.

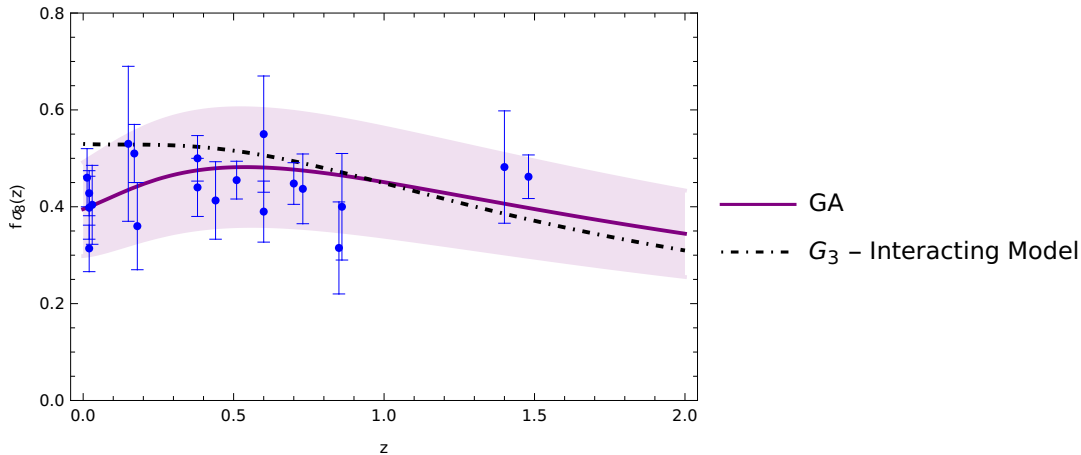


FIG. 5. This plot shows the function generated by the genetic algorithm Eq. (8.4), the purple line. The purple shaded region is the 1σ error bar generated. The dotted-dashed black line is the $f\sigma_8$ curve predicted by the theory.

work by introducing the model in the section II. In the literature, the momentum transfer interacting model is usually introduced by adding the term $f(Z)$ to the Lagrangian. However, we know that the most general scalar tensor theory is described by Horndeski theory and degenerate higher order scalar tensor theory. When including the interaction with dark matter, there is no restriction to have a term like $F(Z)\nabla_\mu\nabla^\mu\phi$.

Then in section III assuming the homogeneous and isotropic flat FLRW metric, we find the background equations of motion. We assume that the theory is shift symmetric, and then the expansion is driven by the kinetic term. Then we proceed to study the ghost conditions for the propagating modes, in section IV. We have two standard tensor modes and one additional scalar mode, which is responsible for the accelerated expansion of the universe, other than the matter scalar modes arising from the matter action. We find the no-ghost condition and the Laplace instability conditions for this model.

In section V, we find the linear perturbation equations of motion in Newtonian gauge. We can see from the dark matter equations of motion that the continuity equation is not modified, rather the Euler equation is modified. This indicates the interaction is only a momentum transfer. Using the linear perturbation equation, we find the evolution of the baryonic and cold dark matter over-densities in the QSA limit in section VI. We found that the gravitational couplings to the baryonic and cold dark matter over-densities are modified.

After deriving the analytic calculation, we introduce a concrete model in the section VII. This model behaves as a tracking solution, that is $\dot{\phi}H = \text{constant}$. Using this concrete model after introducing a field redefinitions, we solve the background equations of motion numerically, and plot the behaviours of the background quantities like Ω_b , Ω_c , Ω_r and Ω_{DE} , which is shown in the figure 1. Then we study the behaviour of the no-ghost and Laplacian instability conditions with the concrete model along the evolution of the universe, figure 2.

Then we solved the equations of motion for the over-densities of baryon and the cold dark matter numerically. The resulting behaviour is shown in the figure 3. In section VIII we move to test the model with the $H(z)$ data and the RSD data ($f\sigma_8$) given in the table I and II, respectively using the genetic algorithm. The resulting figure of background test $H(z)$ data is given in the figure 4. In the figure 4, it is clear that $H(z)$ function of the model we have introduced is well inside the 1σ region of the error bar predicted by the genetic algorithm. For the perturbation, that is for the RSD data, the resulting figure is shown in 5. We found that towards the redshift close to today the value of $f\sigma_8$ lies outside the 1σ region inferred by the genetic algorithm pipeline using the data provided. This enhanced growth is due to the fact that the ratio of the effective gravitational coupling to the G_N grows towards the dark energy domination era as shown in the figure 6. Even though, we find a less preference of this model with $f\sigma_8$ data, we have only tested the model with only one value to the new parameter γ , corresponds to the new interaction we have introduced. To completely rule out this model (at the level of background and the linear perturbation), we need to confront the model with other cosmological data that are currently available from cosmic microwave background radiation and the large scale structures. In other words, we need to do an MCMC simulation and make the parameter estimation with this model.

There are several future directions that are interesting to pursue, gaining intuitions from the current work. One direction is to generalize the concrete model to a general tracker solution with $\dot{\phi}H^p = \text{constant}$ as explored in [46], and following similar analysis and see if the new parameter p can help in reducing the $f\sigma_8$ in to 1σ region of the genetic algorithm pipeline, using the same data. Another direction is to generalise the interacting model itself as studied in the context of Horndeski theory [73]. Then it would be interesting to see the behavior of the $f\sigma_8$. Even though, we did not see any additional propagating modes on the perturbation around the FLRW background, it would be interesting to see if any spurious modes are present in this model. One approach is to do a perturbation analysis on the Bianchi type I spacetime as done in [74–76]. Another obvious direction is to study the constraints of this model by implementing the Einstein - Boltzmann code and confront with the cosmological data. It is also interesting to study the constraints of this new model with integrated Sachs-Wolfe effect and the large scale structure cross correlation data [77, 78], which is a powerful tool to constraint the dark energy models.

ACKNOWLEDGMENTS

The authors acknowledge the Mahidol University International Postdoctoral Fellowship Grant.

Appendix A: Expression for Γ_{cc} , Γ_{cb} , G_{cb} , and G_{cc}

In this appendix we give the expression for Γ_{cc} , Γ_{cb} , G_{cb} , and G_{cc} . Since these expressions are very lengthy, we write down the terms only in the leading order of the interaction term.

$$\Gamma_{cc} = 1 + \Upsilon + \mathcal{O}[F(Z)^2] + \dots \quad (\text{A1})$$

where

$$\Upsilon = \frac{-3H\dot{\phi}^2\ddot{\phi}F_{,ZZ} - \dot{\phi}\ddot{\phi}^2F_{,ZZ} - 3\dot{H}\dot{\phi}^2F_{,Z} - 9H^2\dot{\phi}^2F_{,Z} - 9H\dot{\phi}\ddot{\phi}F_{,Z} - \frac{d^3\phi}{dt^3}\dot{\phi}F_{,Z} - \ddot{\phi}^2F_{,Z}}{2H\rho_c}. \quad (\text{A2})$$

$$\Gamma_{cb} \equiv \frac{\rho_b \dot{\phi}^2 F_{,z} G_{,X} (3H\dot{\phi} + \ddot{\phi})}{\rho_c (2\alpha_1 M_{\text{P}}^2 - 2M_{\text{P}}^2 \dot{\phi}^2 \ddot{\phi} G_{,XX} - 8M_{\text{P}}^2 H \dot{\phi} G_{,X} - 4M_{\text{P}}^2 \ddot{\phi} G_{,X} + \dot{\phi}^4 G_{,X}^2)} + \mathcal{O}[F(Z)^2] + \dots \quad (\text{A3})$$

$$G_{cc}/G_N = G_{G_3} \left[1 + \frac{\mathcal{C}_1}{G_{G_3}} \mathcal{D} \right] + \mathcal{O}[F(Z)^2] + \dots, \quad G_{cb}/G_N = G_{G_3} \left[1 + \frac{\mathcal{C}_2}{G_{G_3}} \mathcal{D} \right] + \mathcal{O}[F(Z)^2] + \dots, \quad (\text{A4})$$

where

$$G_{G_3} \equiv \frac{2M_{\text{P}}^2 (\alpha_1 - \dot{\phi}^2 \ddot{\phi} G_{,XX} - 4H\dot{\phi} G_{,X} - 2\ddot{\phi} G_{,X})}{2M_{\text{P}}^2 (\alpha_1 - \dot{\phi}^2 \ddot{\phi} G_{,XX}) - 8M_{\text{P}}^2 H \dot{\phi} G_{,X} - 4M_{\text{P}}^2 \ddot{\phi} G_{,X} + \dot{\phi}^4 G_{,X}^2}, \quad (\text{A5})$$

$$\mathcal{D} \equiv \left[\alpha_1 + \dot{\phi}^2 \ddot{\phi} (-G_{,XX}) - 4H\dot{\phi} G_{,X} - 2\ddot{\phi} G_{,X} \right] \left[2M_{\text{P}}^2 (\alpha_1 - \dot{\phi}^2 \ddot{\phi} G_{,XX}) - 8M_{\text{P}}^2 H \dot{\phi} G_{,X} - 4M_{\text{P}}^2 \ddot{\phi} G_{,X} + \dot{\phi}^4 G_{,X}^2 \right] \quad (\text{A6})$$

$$\begin{aligned} \mathcal{C}_1 \equiv & -\frac{6F_{,z} G_{,X}^3 \dot{\phi}^7}{M_{\text{P}}^2 \Omega_c} - \frac{F_{,z} G_{,X}^3 \dot{H} \dot{\phi}^7}{M_{\text{P}}^2 H^2 \Omega_c} - \frac{G_{,X}^3 F_{,ZZ} \ddot{\phi} \dot{\phi}^7}{M_{\text{P}}^2 H \Omega_c} + \frac{\alpha_1 F_{,z} G_{,X}^2 \dot{\phi}^6}{M_{\text{P}}^2 H \Omega_c} + \frac{4F_{,z} G_{,XX}^2 \ddot{\phi}^2 \dot{\phi}^6}{H \Omega_c} - \frac{G_{,X}^3 F_{,ZZ} \ddot{\phi}^2 \dot{\phi}^6}{3M_{\text{P}}^2 H^2 \Omega_c} \\ & - \frac{3F_{,z} G_{,X}^3 \ddot{\phi} \dot{\phi}^6}{M_{\text{P}}^2 H \Omega_c} - \frac{2F_{,z} G_{,X} \ddot{\phi}^2 G_{,XXX} \dot{\phi}^6}{H \Omega_c} - \frac{F_{,z} G_{,X}^3 \frac{d^3 \phi}{dt^3} \dot{\phi}^6}{3M_{\text{P}}^2 H^2 \Omega_c} + \frac{4F_{,z} G_{,XX}^2 \ddot{\phi}^3 \dot{\phi}^5}{3H^2 \Omega_c} + \frac{2G_{,X} F_{,ZZ} G_{,XX} \ddot{\phi}^2 \dot{\phi}^5}{H \Omega_c} \\ & + \frac{\alpha_1 F_{,z} G_{,X}^2 \ddot{\phi} \dot{\phi}^5}{3M_{\text{P}}^2 H^2 \Omega_c} + \frac{20F_{,z} G_{,X} G_{,XX} \ddot{\phi} \dot{\phi}^5}{\Omega_c} - 2F_{,z} G_{,X} G_{,XX} \ddot{\phi} \dot{\phi}^5 + \frac{2F_{,z} G_{,X} \dot{H} G_{,XX} \ddot{\phi} \dot{\phi}^5}{H^2 \Omega_c} - \frac{2F_{,z} G_{,X} \ddot{\phi}^3 G_{,XXX} \dot{\phi}^5}{3H^2 \Omega_c} \\ & - \frac{2F_{,z} G_{,X} G_{,XX} \frac{d^3 \phi}{dt^3} \dot{\phi}^5}{H \Omega_c} + \frac{2G_{,X} F_{,ZZ} G_{,XX} \ddot{\phi}^3 \dot{\phi}^4}{3H^2 \Omega_c} - 7HF_{,z} G_{,X}^2 \dot{\phi}^4 - \frac{6HF_{,z} G_{,X}^2 \dot{\phi}^4}{\Omega_c} + \frac{50F_{,z} G_{,X} G_{,XX} \ddot{\phi}^2 \dot{\phi}^4}{3H \Omega_c} \\ & + \frac{8G_{,X}^2 F_{,ZZ} \ddot{\phi} \dot{\phi}^4}{\Omega_c} + G_{,X}^2 F_{,ZZ} \ddot{\phi} \dot{\phi}^4 - \frac{6\alpha_1 F_{,z} G_{,XX} \ddot{\phi} \dot{\phi}^4}{H \Omega_c} + \frac{48N_c^6 F_{,z} G_{,X}^2 \rho_{c,\tilde{n}\tilde{n}\tilde{n}} (\tilde{n}) \dot{\phi}^4}{M_{\text{P}}^2 a^{18} H \Omega_c^2} + \frac{8F_{,z} G_{,X} G_{,XX} \ddot{\phi}^3 \dot{\phi}^3}{3H^2 \Omega_c} \\ & + \frac{20G_{,X}^2 F_{,ZZ} \ddot{\phi}^2 \dot{\phi}^3}{3H \Omega_c} - \frac{2\alpha_1 F_{,z} G_{,XX} \ddot{\phi}^2 \dot{\phi}^3}{H^2 \Omega_c} + 2\alpha_1 F_{,z} G_{,X} \dot{\phi}^3 - \frac{20\alpha_1 F_{,z} G_{,X} \dot{\phi}^3}{\Omega_c} - \frac{2\alpha_1 F_{,z} G_{,X} \dot{H} \dot{\phi}^3}{H^2 \Omega_c} \\ & + \frac{54F_{,z} G_{,X}^2 \ddot{\phi} \dot{\phi}^3}{\Omega_c} - 4F_{,z} G_{,X}^2 \ddot{\phi} \dot{\phi}^3 + \frac{4F_{,z} G_{,X}^2 \dot{H} \ddot{\phi} \dot{\phi}^3}{3H^2 \Omega_c} - \frac{2\alpha_1 G_{,X} F_{,ZZ} \ddot{\phi} \dot{\phi}^3}{H \Omega_c} + \frac{16N_c^6 F_{,z} G_{,X}^2 \ddot{\phi} \rho_{c,\tilde{n}\tilde{n}\tilde{n}} (\tilde{n}) \dot{\phi}^3}{M_{\text{P}}^2 a^{18} H^2 \Omega_c^2} \\ & - \frac{4F_{,z} G_{,X}^2 \frac{d^3 \phi}{dt^3} \dot{\phi}^3}{3H \Omega_c} + \frac{4G_{,X}^2 F_{,ZZ} \ddot{\phi}^3 \dot{\phi}^2}{3H^2 \Omega_c} + \frac{36F_{,z} G_{,X}^2 \ddot{\phi}^2 \dot{\phi}^2}{H \Omega_c} - \frac{2\alpha_1 G_{,X} F_{,ZZ} \ddot{\phi}^2 \dot{\phi}^2}{3H^2 \Omega_c} + \frac{2\alpha_1^2 F_{,z} \dot{\phi}^2}{H \Omega_c} - \frac{62\alpha_1 F_{,z} G_{,X} \ddot{\phi} \dot{\phi}^2}{3H \Omega_c} \\ & + \frac{108M_{\text{P}}^2 HF_{,z} G_{,XX} \ddot{\phi} \dot{\phi}^2}{\Omega_c} - \frac{96N_c^6 F_{,z} G_{,XX} \ddot{\phi} \rho_{c,\tilde{n}\tilde{n}\tilde{n}} (\tilde{n}) \dot{\phi}^2}{a^{18} H \Omega_c^2} - \frac{2\alpha_1 F_{,z} G_{,X} \frac{d^3 \phi}{dt^3} \dot{\phi}^2}{3H^2 \Omega_c} + \frac{16F_{,z} G_{,X}^2 \ddot{\phi}^3 \dot{\phi}}{3H^2 \Omega_c} - \frac{4\alpha_1 F_{,z} G_{,X} \ddot{\phi}^2 \dot{\phi}}{H^2 \Omega_c} \\ & + \frac{36M_{\text{P}}^2 F_{,z} G_{,XX} \ddot{\phi}^2 \dot{\phi}}{\Omega_c} + \frac{432M_{\text{P}}^2 H^2 F_{,z} G_{,X} \dot{\phi}}{\Omega_c} + \frac{2\alpha_1^2 F_{,z} \ddot{\phi} \dot{\phi}}{3H^2 \Omega_c} - \frac{32N_c^6 F_{,z} G_{,XX} \ddot{\phi}^2 \rho_{c,\tilde{n}\tilde{n}\tilde{n}} (\tilde{n}) \dot{\phi}}{a^{18} H^2 \Omega_c^2} \\ & - \frac{384N_c^6 F_{,z} G_{,X} \rho_{c,\tilde{n}\tilde{n}\tilde{n}} (\tilde{n}) \dot{\phi}}{a^{18} \Omega_c^2} - \frac{108\alpha_1 M_{\text{P}}^2 HF_{,z}}{\Omega_c} + \frac{360M_{\text{P}}^2 HF_{,z} G_{,X} \ddot{\phi}}{\Omega_c} + \frac{96\alpha_1 N_c^6 F_{,z} \rho_{c,\tilde{n}\tilde{n}\tilde{n}} (\tilde{n})}{a^{18} H \Omega_c^2} \\ & - \frac{320N_c^6 F_{,z} G_{,X} \ddot{\phi} \rho_{c,\tilde{n}\tilde{n}\tilde{n}} (\tilde{n})}{a^{18} H \Omega_c^2} + \frac{72M_{\text{P}}^2 F_{,z} G_{,X} \ddot{\phi}^2}{\Omega_c \dot{\phi}} - \frac{36\alpha_1 M_{\text{P}}^2 F_{,z} \ddot{\phi}}{\Omega_c \dot{\phi}} - \frac{64N_c^6 F_{,z} G_{,X} \ddot{\phi}^2 \rho_{c,\tilde{n}\tilde{n}\tilde{n}} (\tilde{n})}{a^{18} H^2 \Omega_c^2 \dot{\phi}} + \frac{32\alpha_1 N_c^6 F_{,z} \ddot{\phi} \rho_{c,\tilde{n}\tilde{n}\tilde{n}} (\tilde{n})}{a^{18} H^2 \Omega_c^2 \dot{\phi}} \end{aligned} \quad (\text{A7})$$

$$\begin{aligned}
\mathcal{C}_2 \equiv & -\frac{6F_{,Z}G_{,X}^3\dot{\phi}^7}{M_{\text{P}}^2\Omega_c} - \frac{F_{,Z}G_{,X}^3\dot{H}\dot{\phi}^7}{M_{\text{P}}^2H^2\Omega_c} - \frac{G_{,X}^3F_{,ZZ}\ddot{\phi}\dot{\phi}^7}{M_{\text{P}}^2H\Omega_c} + \frac{\alpha_1F_{,Z}G_{,X}^2\dot{\phi}^6}{M_{\text{P}}^2H\Omega_c} + \frac{4F_{,Z}G_{,XX}^2\ddot{\phi}^2\dot{\phi}^6}{H\Omega_c} - \frac{G_{,X}^3F_{,ZZ}\ddot{\phi}^2\dot{\phi}^6}{3M_{\text{P}}^2H^2\Omega_c} \\
& - \frac{3F_{,Z}G_{,X}^3\ddot{\phi}\dot{\phi}^6}{M_{\text{P}}^2H\Omega_c} - \frac{2F_{,Z}G_{,X}\ddot{\phi}^2G_{,XXX}\dot{\phi}^6}{H\Omega_c} - \frac{F_{,Z}G_{,X}^3\frac{d^3\phi}{dt^3}\dot{\phi}^6}{3M_{\text{P}}^2H^2\Omega_c} + \frac{4F_{,Z}G_{,XX}^2\ddot{\phi}^3\dot{\phi}^5}{3H^2\Omega_c} + \frac{2G_{,XF,ZZ}G_{,XX}\ddot{\phi}^2\dot{\phi}^5}{H\Omega_c} \\
& + \frac{\alpha_1F_{,Z}G_{,X}^2\ddot{\phi}\dot{\phi}^5}{3M_{\text{P}}^2H^2\Omega_c} + \frac{20F_{,Z}G_{,X}G_{,XX}\ddot{\phi}\dot{\phi}^5}{\Omega_c} - 2F_{,Z}G_{,X}G_{,XX}\ddot{\phi}\dot{\phi}^5 + \frac{2F_{,Z}G_{,X}\dot{H}G_{,XX}\ddot{\phi}\dot{\phi}^5}{H^2\Omega_c} - \frac{2F_{,Z}G_{,X}\ddot{\phi}^3G_{,XXX}\dot{\phi}^5}{3H^2\Omega_c} \\
& - \frac{2F_{,Z}G_{,X}G_{,XX}\frac{d^3\phi}{dt^3}\dot{\phi}^5}{H\Omega_c} + \frac{2G_{,XF,ZZ}G_{,XX}\ddot{\phi}^3\dot{\phi}^4}{3H^2\Omega_c} - 7HF_{,Z}G_{,Z}^2\dot{\phi}^4 + \frac{48HF_{,Z}G_{,X}^2\dot{\phi}^4}{\Omega_c} + \frac{50F_{,Z}G_{,X}G_{,XX}\ddot{\phi}^2\dot{\phi}^4}{3H\Omega_c} \\
& + \frac{8G_{,XF,ZZ}^2\ddot{\phi}\dot{\phi}^4}{\Omega_c} + G_{,ZF,ZZ}^2\ddot{\phi}\dot{\phi}^4 - \frac{6\alpha_1F_{,Z}G_{,XX}\ddot{\phi}\dot{\phi}^4}{H\Omega_c} + \frac{6N_{\text{b}}^3F_{,Z}G_{,X}^2\rho_{,n_{\text{b}}n_{\text{b}}n_{\text{b}}}(n_{\text{b}})\dot{\phi}^4}{M_{\text{P}}^2a^9H\Omega_{\text{b}}\Omega_c} + \frac{8F_{,Z}G_{,X}G_{,XX}\ddot{\phi}^3\dot{\phi}^3}{3H^2\Omega_c} \\
& + \frac{20G_{,XF,ZZ}^2\ddot{\phi}^2\dot{\phi}^3}{3H\Omega_c} - \frac{2\alpha_1F_{,Z}G_{,XX}\ddot{\phi}^2\dot{\phi}^3}{H^2\Omega_c} + 2\alpha_1F_{,Z}G_{,X}\dot{\phi}^3 - \frac{20\alpha_1F_{,Z}G_{,X}\dot{\phi}^3}{\Omega_c} - \frac{2\alpha_1F_{,Z}G_{,X}\dot{H}\dot{\phi}^3}{H^2\Omega_c} + \frac{72F_{,Z}G_{,X}^2\ddot{\phi}\dot{\phi}^3}{\Omega_c} \\
& - 4F_{,Z}G_{,X}^2\ddot{\phi}\dot{\phi}^3 + \frac{4F_{,Z}G_{,X}^2\dot{H}\ddot{\phi}\dot{\phi}^3}{3H^2\Omega_c} - \frac{2\alpha_1G_{,XF,ZZ}\ddot{\phi}\dot{\phi}^3}{H\Omega_c} + \frac{2N_{\text{b}}^3F_{,Z}G_{,X}^2\ddot{\phi}\rho_{,n_{\text{b}}n_{\text{b}}n_{\text{b}}}(n_{\text{b}})\dot{\phi}^3}{M_{\text{P}}^2a^9H^2\Omega_{\text{b}}\Omega_c} - \frac{4F_{,Z}G_{,X}^2\frac{d^3\phi}{dt^3}\dot{\phi}^3}{3H\Omega_c} \\
& + \frac{4G_{,XF,ZZ}^2\ddot{\phi}^3\dot{\phi}^2}{3H^2\Omega_c} + \frac{36F_{,Z}G_{,X}^2\ddot{\phi}^2\dot{\phi}^2}{H\Omega_c} - \frac{2\alpha_1G_{,XF,ZZ}\ddot{\phi}^2\dot{\phi}^2}{3H^2\Omega_c} + \frac{2\alpha_1^2F_{,Z}\dot{\phi}^2}{H\Omega_c} - \frac{62\alpha_1F_{,Z}G_{,X}\ddot{\phi}\dot{\phi}^2}{3H\Omega_c} \\
& - \frac{12N_{\text{b}}^3F_{,Z}G_{,XX}\ddot{\phi}\rho_{,n_{\text{b}}n_{\text{b}}n_{\text{b}}}(n_{\text{b}})\dot{\phi}^2}{a^9H\Omega_{\text{b}}\Omega_c} - \frac{2\alpha_1F_{,Z}G_{,X}\frac{d^3\phi}{dt^3}\dot{\phi}^2}{3H^2\Omega_c} + \frac{16F_{,Z}G_{,X}^2\ddot{\phi}^3\dot{\phi}}{3H^2\Omega_c} - \frac{4\alpha_1F_{,Z}G_{,X}\ddot{\phi}^2\dot{\phi}}{H^2\Omega_c} + \frac{2\alpha_1^2F_{,Z}\ddot{\phi}\dot{\phi}}{3H^2\Omega_c} \\
& - \frac{4N_{\text{b}}^3F_{,Z}G_{,XX}\ddot{\phi}^2\rho_{,n_{\text{b}}n_{\text{b}}n_{\text{b}}}(n_{\text{b}})\dot{\phi}}{a^9H^2\Omega_{\text{b}}\Omega_c} - \frac{48N_{\text{b}}^3F_{,Z}G_{,X}\rho_{,n_{\text{b}}n_{\text{b}}n_{\text{b}}}(n_{\text{b}})\dot{\phi}}{a^9\Omega_{\text{b}}\Omega_c} + \frac{12\alpha_1N_{\text{b}}^3F_{,Z}\rho_{,n_{\text{b}}n_{\text{b}}n_{\text{b}}}(n_{\text{b}})}{a^9H\Omega_{\text{b}}\Omega_c} \\
& - \frac{40N_{\text{b}}^3F_{,Z}G_{,X}\ddot{\phi}\rho_{,n_{\text{b}}n_{\text{b}}n_{\text{b}}}(n_{\text{b}})}{a^9H\Omega_{\text{b}}\Omega_c} - \frac{8N_{\text{b}}^3F_{,Z}G_{,X}\ddot{\phi}^2\rho_{,n_{\text{b}}n_{\text{b}}n_{\text{b}}}(n_{\text{b}})}{a^9H^2\Omega_{\text{b}}\Omega_c\dot{\phi}} + \frac{4\alpha_1N_{\text{b}}^3F_{,Z}\ddot{\phi}\rho_{,n_{\text{b}}n_{\text{b}}n_{\text{b}}}(n_{\text{b}})}{a^9H^2\Omega_{\text{b}}\Omega_c\dot{\phi}} \tag{A8}
\end{aligned}$$

Appendix B: Behaviour of G_{cc} and G_{bb} along the redshift

In this appendix we show the behaviour of the G_{cc}/G_N and G_{bb}/G_N along the variable $\mathcal{N} = \ln(a)$. As we can see that there is enhancement in the ratio between $G_{cc}(G_{bb})$ and G_N in the dark energy domination era.

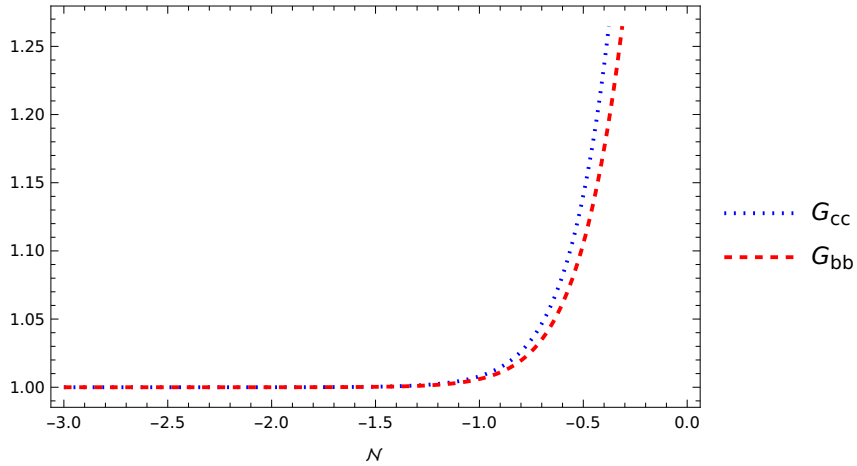


FIG. 6. The behaviour of effective gravitational coupling to the cold dark matter and the baryon G_{cc} and G_{bb} respectively.

-
- [1] SUPERNOVA SEARCH TEAM collaboration, *Observational evidence from supernovae for an accelerating universe and a cosmological constant*, *Astron. J.* **116** (1998) 1009 [astro-ph/9805201].
- [2] SUPERNOVA COSMOLOGY PROJECT collaboration, *Measurements of Ω and Λ from 42 High Redshift Supernovae*, *Astrophys. J.* **517** (1999) 565 [astro-ph/9812133].
- [3] BOOMERANG collaboration, *A Flat universe from high resolution maps of the cosmic microwave background radiation*, *Nature* **404** (2000) 955 [astro-ph/0004404].
- [4] WMAP collaboration, *First year Wilkinson Microwave Anisotropy Probe (WMAP) observations: Determination of cosmological parameters*, *Astrophys. J. Suppl.* **148** (2003) 175 [astro-ph/0302209].
- [5] WMAP collaboration, *Five-Year Wilkinson Microwave Anisotropy Probe (WMAP) Observations: Likelihoods and Parameters from the WMAP data*, *Astrophys. J. Suppl.* **180** (2009) 306 [0803.0586].
- [6] PLANCK collaboration, *Planck 2013 results. XVI. Cosmological parameters*, *Astron. Astrophys.* **571** (2014) A16 [1303.5076].
- [7] PLANCK collaboration, *Planck 2018 results. VI. Cosmological parameters*, *Astron. Astrophys.* **641** (2020) A6 [1807.06209].
- [8] A.G. Riess, L. Macri, S. Casertano, H. Lampeitl, H.C. Ferguson, A.V. Filippenko et al., *A 3% Solution: Determination of the Hubble Constant with the Hubble Space Telescope and Wide Field Camera 3*, *Astrophys. J.* **730** (2011) 119 [1103.2976].
- [9] A.G. Riess et al., *A Comprehensive Measurement of the Local Value of the Hubble Constant with 1 km s⁻¹ Mpc⁻¹ Uncertainty from the Hubble Space Telescope and the SH0ES Team*, *Astrophys. J. Lett.* **934** (2022) L7 [2112.04510].
- [10] DES collaboration, *Dark Energy Survey Year 3 results: Cosmology from cosmic shear and robustness to data calibration*, *Phys. Rev. D* **105** (2022) 023514 [2105.13543].
- [11] S. Tsujikawa, *Quintessence: A Review*, *Class. Quant. Grav.* **30** (2013) 214003 [1304.1961].
- [12] C. Lin and S. Mukohyama, *A Class of Minimally Modified Gravity Theories*, *JCAP* **10** (2017) 033 [1708.03757].
- [13] S. Mukohyama and K. Noui, *Minimally Modified Gravity: a Hamiltonian Construction*, *JCAP* **07** (2019) 049 [1905.02000].
- [14] A. De Felice, A. Doll and S. Mukohyama, *A theory of type-II minimally modified gravity*, *JCAP* **09** (2020) 034 [2004.12549].
- [15] A. De Felice, S. Mukohyama and M.C. Pookkillath, *Addressing H_0 tension by means of Λ CDM*, *Phys. Lett. B* **816** (2021) 136201 [2009.08718].
- [16] K. Aoki, A. De Felice, S. Mukohyama, K. Noui, M. Oliosi and M.C. Pookkillath, *Minimally modified gravity fitting Planck data better than Λ CDM*, *Eur. Phys. J. C* **80** (2020) 708 [2005.13972].
- [17] N. Afshordi, D.J.H. Chung and G. Geshnizjani, *Cuscuton: A Causal Field Theory with an Infinite Speed of Sound*, *Phys. Rev. D* **75** (2007) 083513 [hep-th/0609150].
- [18] M. Mylova and N. Afshordi, *Effective cuscuton theory*, *JHEP* **04** (2024) 144 [2312.06066].
- [19] C. Armendariz-Picon, V.F. Mukhanov and P.J. Steinhardt, *Essentials of k essence*, *Phys. Rev. D* **63** (2001) 103510 [astro-ph/0006373].
- [20] G.W. Horndeski, *Second-order scalar-tensor field equations in a four-dimensional space*, *Int. J. Theor. Phys.* **10** (1974) 363.
- [21] J. Gleyzes, D. Langlois, F. Piazza and F. Vernizzi, *Healthy theories beyond Horndeski*, *Phys. Rev. Lett.* **114** (2015) 211101 [1404.6495].
- [22] D. Langlois and K. Noui, *Degenerate higher derivative theories beyond Horndeski: evading the Ostrogradski instability*, *JCAP* **02** (2016) 034 [1510.06930].
- [23] C. Armendariz-Picon, *Could dark energy be vector-like?*, *JCAP* **07** (2004) 007 [astro-ph/0405267].
- [24] L. Heisenberg, *Generalization of the Proca Action*, *JCAP* **05** (2014) 015 [1402.7026].
- [25] C. de Rham and V. Pozsgay, *New class of Proca interactions*, *Phys. Rev. D* **102** (2020) 083508 [2003.13773].
- [26] A. De Felice, L. Heisenberg, R. Kase, S. Mukohyama, S. Tsujikawa and Y.-l. Zhang, *Cosmology in generalized Proca theories*, *JCAP* **06** (2016) 048 [1603.05806].
- [27] A. De Felice, C.-Q. Geng, M.C. Pookkillath and L. Yin, *Reducing the H_0 tension with generalized Proca theory*, *JCAP* **08** (2020) 038 [2002.06782].
- [28] C. de Rham, S. Garcia-Saenz, L. Heisenberg and V. Pozsgay, *Cosmology of Extended Proca-Nuevo*, *JCAP* **03** (2022) 053 [2110.14327].
- [29] A. Pourtsidou, C. Skordis and E.J. Copeland, *Models of dark matter coupled to dark energy*, *Phys. Rev. D* **88** (2013) 083505 [1307.0458].
- [30] R. Kase and S. Tsujikawa, *General formulation of cosmological perturbations in scalar-tensor dark energy coupled to dark matter*, *JCAP* **11** (2020) 032 [2005.13809].
- [31] A. De Felice, S. Nakamura and S. Tsujikawa, *Suppressed cosmic growth in coupled vector-tensor theories*, *Phys. Rev. D* **102** (2020) 063531 [2004.09384].
- [32] M.C. Pookkillath and K. Koyama, *Theory of interacting vector dark energy and fluid*, **2405.06565**.
- [33] E. Di Valentino, O. Mena, S. Pan, L. Visinelli, W. Yang, A. Melchiorri et al., *In the realm of the Hubble tension—a review of solutions*, *Class. Quant. Grav.* **38** (2021) 153001 [2103.01183].

- [34] E. Di Valentino, A. Melchiorri, O. Mena and S. Vagnozzi, *Interacting dark energy in the early 2020s: A promising solution to the H_0 and cosmic shear tensions*, *Phys. Dark Univ.* **30** (2020) 100666 [1908.04281].
- [35] J. Beltrán Jiménez, D. Bettoni, D. Figueruelo, F.A. Teppa Pannia and S. Tsujikawa, *Probing elastic interactions in the dark sector and the role of $S8$* , *Phys. Rev. D* **104** (2021) 103503 [2106.11222].
- [36] X.-L. Luo, J. Feng and H.-H. Zhang, *A genetic algorithm for astroparticle physics studies*, *Comput. Phys. Commun.* **250** (2020) 106818 [1907.01090].
- [37] M. Ho, M.M. Rau, M. Ntampaka, A. Farahi, H. Trac and B. Poczós, *A Robust and Efficient Deep Learning Method for Dynamical Mass Measurements of Galaxy Clusters*, *Astrophys. J.* **887** (2019) 25 [1902.05950].
- [38] C. Bogdanos and S. Nesseris, *Genetic Algorithms and Supernovae Type Ia Analysis*, *JCAP* **05** (2009) 006 [0903.2805].
- [39] S. Nesseris and A. Shafieloo, *A model independent null test on the cosmological constant*, *Mon. Not. Roy. Astron. Soc.* **408** (2010) 1879 [1004.0960].
- [40] S. Nesseris and J. García-Bellido, *A new perspective on Dark Energy modeling via Genetic Algorithms*, *JCAP* **11** (2012) 033 [1205.0364].
- [41] S. Nesseris and J. García-Bellido, *Comparative analysis of model-independent methods for exploring the nature of dark energy*, *Phys. Rev. D* **88** (2013) 063521 [1306.4885].
- [42] D. Sapone, E. Majerotto and S. Nesseris, *Curvature versus distances: Testing the FLRW cosmology*, *Phys. Rev. D* **90** (2014) 023012 [1402.2236].
- [43] R. Arjona and S. Nesseris, *What can Machine Learning tell us about the background expansion of the Universe?*, *Phys. Rev. D* **101** (2020) 123525 [1910.01529].
- [44] G. Alestas, L. Kazantzidis and S. Nesseris, *Machine learning constraints on deviations from general relativity from the large scale structure of the Universe*, *Phys. Rev. D* **106** (2022) 103519 [2209.12799].
- [45] T. Clemson, K. Koyama, G.-B. Zhao, R. Maartens and J. Valiviita, *Interacting Dark Energy – constraints and degeneracies*, *Phys. Rev. D* **85** (2012) 043007 [1109.6234].
- [46] A. De Felice and S. Tsujikawa, *Conditions for the cosmological viability of the most general scalar-tensor theories and their applications to extended Galileon dark energy models*, *JCAP* **02** (2012) 007 [1110.3878].
- [47] A. De Felice and S. Tsujikawa, *Cosmology of a covariant Galileon field*, *Phys. Rev. Lett.* **105** (2010) 111301 [1007.2700].
- [48] S. Nesseris and J. García-Bellido, *A new perspective on dark energy modeling via genetic algorithms*, *JCAP* **2012** (2012) 033 [1205.0364].
- [49] D. Stern, R. Jimenez, L. Verde, M. Kamionkowski and S.A. Stanford, *Cosmic Chronometers: Constraining the Equation of State of Dark Energy. I: $H(z)$ Measurements*, *JCAP* **02** (2010) 008 [0907.3149].
- [50] C. Blake et al., *The WiggleZ Dark Energy Survey: Joint measurements of the expansion and growth history at $z < 1$* , *Mon. Not. Roy. Astron. Soc.* **425** (2012) 405 [1204.3674].
- [51] M. Moresco et al., *Improved constraints on the expansion rate of the Universe up to $z \sim 1.1$ from the spectroscopic evolution of cosmic chronometers*, *JCAP* **08** (2012) 006 [1201.3609].
- [52] C.-H. Chuang and Y. Wang, *Modeling the Anisotropic Two-Point Galaxy Correlation Function on Small Scales and Improved Measurements of $H(z)$, $D_A(z)$, and $\beta(z)$ from the Sloan Digital Sky Survey DR7 Luminous Red Galaxies*, *Mon. Not. Roy. Astron. Soc.* **435** (2013) 255 [1209.0210].
- [53] C. Zhang, H. Zhang, S. Yuan, T.-J. Zhang and Y.-C. Sun, *Four new observational $H(z)$ data from luminous red galaxies in the Sloan Digital Sky Survey data release seven*, *Res. Astron. Astrophys.* **14** (2014) 1221 [1207.4541].
- [54] BOSS collaboration, *The clustering of galaxies in the SDSS-III Baryon Oscillation Spectroscopic Survey: baryon acoustic oscillations in the Data Releases 10 and 11 Galaxy samples*, *Mon. Not. Roy. Astron. Soc.* **441** (2014) 24 [1312.4877].
- [55] BOSS collaboration, *Baryon acoustic oscillations in the Ly α forest of BOSS DR11 quasars*, *Astron. Astrophys.* **574** (2015) A59 [1404.1801].
- [56] M. Moresco, *Raising the bar: new constraints on the Hubble parameter with cosmic chronometers at $z \sim 2$* , *Mon. Not. Roy. Astron. Soc.* **450** (2015) L16 [1503.01116].
- [57] M. Moresco, L. Pozzetti, A. Cimatti, R. Jimenez, C. Maraston, L. Verde et al., *A 6% measurement of the Hubble parameter at $z \sim 0.45$: direct evidence of the epoch of cosmic re-acceleration*, *JCAP* **05** (2016) 014 [1601.01701].
- [58] A.L. Ratsimbazafy, S.I. Loubser, S.M. Crawford, C.M. Cress, B.A. Bassett, R.C. Nichol et al., *Age-dating Luminous Red Galaxies observed with the Southern African Large Telescope*, *Mon. Not. Roy. Astron. Soc.* **467** (2017) 3239 [1702.00418].
- [59] N. Borghi, M. Moresco and A. Cimatti, *Toward a Better Understanding of Cosmic Chronometers: A New Measurement of $H(z)$ at $z \sim 0.7$* , *Astrophys. J. Lett.* **928** (2022) L4 [2110.04304].
- [60] K. Jiao, N. Borghi, M. Moresco and T.-J. Zhang, *New Observational $H(z)$ Data from Full-spectrum Fitting of Cosmic Chronometers in the LEGA-C Survey*, *Astrophys. J. Suppl.* **265** (2023) 48 [2205.05701].
- [61] R. Arjona and S. Nesseris, *Hints of dark energy anisotropic stress using Machine Learning*, *JCAP* **11** (2020) 042 [2001.11420].
- [62] Y.-S. Song and W.J. Percival, *Reconstructing the history of structure formation using Redshift Distortions*, *JCAP* **10** (2009) 004 [0807.0810].
- [63] M. Davis, A. Nusser, K. Masters, C. Springob, J.P. Huchra and G. Lemson, *Local Gravity versus Local Velocity: Solutions for β and nonlinear bias*, *Mon. Not. Roy. Astron. Soc.* **413** (2011) 2906 [1011.3114].
- [64] M.J. Hudson and S.J. Turnbull, *The growth rate of cosmic structure from peculiar velocities at low and high redshifts*, *Astrophys. J. Lett.* **751** (2013) L30 [1203.4814].
- [65] S.J. Turnbull, M.J. Hudson, H.A. Feldman, M. Hicken, R.P. Kirshner and R. Watkins, *Cosmic flows in the nearby universe from Type Ia Supernovae*, *Mon. Not. Roy. Astron. Soc.* **420** (2012) 447 [1111.0631].

- [66] C. Blake et al., *Galaxy And Mass Assembly (GAMA): improved cosmic growth measurements using multiple tracers of large-scale structure*, *Mon. Not. Roy. Astron. Soc.* **436** (2013) 3089 [1309.5556].
- [67] T. Okumura et al., *The Subaru FMOS galaxy redshift survey (FastSound). IV. New constraint on gravity theory from redshift space distortions at $z \sim 1.4$* , *Publ. Astron. Soc. Jap.* **68** (2016) 38 [1511.08083].
- [68] D. Huterer, D. Shafer, D. Scolnic and F. Schmidt, *Testing Λ CDM at the lowest redshifts with SN Ia and galaxy velocities*, *JCAP* **05** (2017) 015 [1611.09862].
- [69] A. Pezzotta et al., *The VIMOS Public Extragalactic Redshift Survey (VIPERS): The growth of structure at $0.5 < z < 1.2$ from redshift-space distortions in the clustering of the PDR-2 final sample*, *Astron. Astrophys.* **604** (2017) A33 [1612.05645].
- [70] F. Qin, C. Howlett and L. Staveley-Smith, *The redshift-space momentum power spectrum – II. Measuring the growth rate from the combined 2MTF and 6dFGSv surveys*, *Mon. Not. Roy. Astron. Soc.* **487** (2019) 5235 [1906.02874].
- [71] F. Avila, A. Bernui, E. de Carvalho and C.P. Novaes, *The growth rate of cosmic structures in the local Universe with the ALFALFA survey*, *Mon. Not. Roy. Astron. Soc.* **505** (2021) 3404 [2105.10583].
- [72] EBOSS collaboration, *Completed SDSS-IV extended Baryon Oscillation Spectroscopic Survey: Cosmological implications from two decades of spectroscopic surveys at the Apache Point Observatory*, *Phys. Rev. D* **103** (2021) 083533 [2007.08991].
- [73] A. De Felice and S. Tsujikawa, *Generalized Galileon cosmology*, *Phys. Rev. D* **84** (2011) 124029 [1008.4236].
- [74] A. De Felice, A.E. Gümrukçüoğlu, C. Lin and S. Mukohyama, *Nonlinear stability of cosmological solutions in massive gravity*, *JCAP* **05** (2013) 035 [1303.4154].
- [75] M.C. Pookkillath, A. De Felice and A.A. Starobinsky, *Anisotropic instability in a higher order gravity theory*, *JCAP* **07** (2020) 041 [2004.03912].
- [76] A. De Felice, R. Kawaguchi, K. Mizui and S. Tsujikawa, *Starobinsky inflation with a quadratic Weyl tensor*, *Phys. Rev. D* **108** (2023) 123524 [2309.01835].
- [77] R. Kimura, T. Kobayashi and K. Yamamoto, *Observational Constraints on Kinetic Gravity Braiding from the Integrated Sachs-Wolfe Effect*, *Phys. Rev. D* **85** (2012) 123503 [1110.3598].
- [78] J.A. Kable, G. Benevento, N. Frusciante, A. De Felice and S. Tsujikawa, *Probing modified gravity with integrated Sachs-Wolfe CMB and galaxy cross-correlations*, *JCAP* **09** (2022) 002 [2111.10432].